THE IIOAB JOURNAL

VOLUME 12 : NO 1 : APRIL 2021 : ISSN 0976-3104

Institute of Integrative Omics and Applied Biotechnology Journal

Dear Esteemed Readers, Authors, and Colleagues,

I hope this letter finds you in good health and high spirits. It is my distinct pleasure to address you as the Editor-in-Chief of Integrative Omics and Applied Biotechnology (IIOAB) Journal, a multidisciplinary scientific journal that has always placed a profound emphasis on nurturing the involvement of young scientists and championing the significance of an interdisciplinary approach.

At Integrative Omics and Applied Biotechnology (IIOAB) Journal, we firmly believe in the transformative power of science and innovation, and we recognize that it is the vigor and enthusiasm of young minds that often drive the most groundbreaking discoveries. We actively encourage students, early-career researchers, and scientists to submit their work and engage in meaningful discourse within the pages of our journal. We take pride in providing a platform for these emerging researchers to share their novel ideas and findings with the broader scientific community.

In today's rapidly evolving scientific landscape, it is increasingly evident that the challenges we face require a collaborative and interdisciplinary approach. The most complex problems demand a diverse set of perspectives and expertise. Integrative Omics and Applied Biotechnology (IIOAB) Journal has consistently promoted and celebrated this multidisciplinary ethos. We believe that by crossing traditional disciplinary boundaries, we can unlock new avenues for discovery, innovation, and progress. This philosophy has been at the heart of our journal's mission, and we remain dedicated to publishing research that exemplifies the power of interdisciplinary collaboration.

Our journal continues to serve as a hub for knowledge exchange, providing a platform for researchers from various fields to come together and share their insights, experiences, and research outcomes. The collaborative spirit within our community is truly inspiring, and I am immensely proud of the role that IIOAB journal plays in fostering such partnerships.

As we move forward, I encourage each and every one of you to continue supporting our mission. Whether you are a seasoned researcher, a young scientist embarking on your career, or a reader with a thirst for knowledge, your involvement in our journal is invaluable. By working together and embracing interdisciplinary perspectives, we can address the most pressing challenges facing humanity, from climate change and public health to technological advancements and social issues.

I would like to extend my gratitude to our authors, reviewers, editorial board members, and readers for their unwavering support. Your dedication is what makes IIOAB Journal the thriving scientific community it is today. Together, we will continue to explore the frontiers of knowledge and pioneer new approaches to solving the world's most complex problems.

Thank you for being a part of our journey, and for your commitment to advancing science through the pages of IIOAB Journal.

Yours sincerely,

Vasco Azevedo

Vasco Azevedo, Editor-in-Chief
Integrative Omics and Applied Biotechnology
(IIOAB) Journal

Prof. Vasco Azevedo
Federal University of Minas Gerais
Brazil

Editor-in-Chief

Integrative Omics and Applied Biotechnology (IIOAB) Journal Editorial Board:

IIOAB JOURNAL

ARTICLE

AN OPTIMAL METAHEURISTIC BASED FEATURE SELECTION WITH DEEP LEARNING MODEL FOR AUTISM SPECTRUM DISORDER DIAGNOSIS AND CLASSIFICATION

Umamaheswari Krishnan[1*], Latha Parthiban[2]

[1]*Department of Computer Science, Bharathiyar University, TN, INDIA*
[2]*Department of Computer Science, Community College, Pondicherry University, INDIA*

ISSN 0976-3104

ABSTRACT

Autism spectrum disorder (ASD) is a neurological disorder defined by a particular set of issues linked to communication, social skill, and repetitive behavior. Recently, machine learning (ML) and healthcare sectors are integrated to determine the presence of several diseases. Therefore, this paper presents a new ASD diagnosis model using quasi oppositional based dragonfly algorithm (DOA) for feature selection (QODF) with deep SAE network (DSAN). The proposed QODF-DSAN model incorporates quasi oppositional based learning (QOBL) concept to increase the convergence rate of DOA. The QODF algorithm is employed for selecting an optimal subset of features. In addition, the DSAN model is applied for classification purposes. In order to ensure the effective performance of the QODF-DSAN model, a set of simulations takes place on three benchmark dataset. The resultant simulation outcome verified the effective classification results with the higher accuracy of 97.60%, 97.87%, and 97.12% on ASD-Children, ASD-Adolescent, and ASD-Adult dataset respectively.

KEY WORDS
ASD, Metaheuristic, Machine learning, Feature selection, Data classification

INTRODUCTION

In general, Autism Spectrum Disorder (ASD) is a neuro developmental infection classified by pervasive defects in social communication, and repeated behaviors, diverse interests, and function. The traditional concepts are relevant to different ailments like autistic infection, Asperger's ailments, and genetic disintegrative disorder [1]. ASD is recently divided as a single disorder with severity level that fails to continue in final edition of Diagnostic and Statistical Manual of Mental Disorders (DSM-5) [1]. The shifting towards a categorical to dimensional method results in well-equipped physicians by applying standardized diagnostic tools which differentiate the signs of DSM-IV disorders [2]. Moreover, DSM-5 is composed of reports with co-occurring situations and age of onset. It modified to ASD diagnostic criteria which facilitates to categorize the subtypes of ASD [3]. As shown by recent diagnostic applications, ASD is one of the heterogeneous infections. The signs of ASD are language disability and skills in alternate developmental applications (adaptive skills and executive performance) [4] which differ in higher value over the examined individuals.

Followed by, onset of symptoms varies from one another that shows delays or plateaus in deployment, and regression of classically obtained achievements. Most of the patients affected with ASD have alternate disorders which are prevalent. ASD is caused for various reasons like genetics and environment functions. It can be examined with genetic variants of ASD cases, and massive number of cases is linked with genes. Moreover, the common rates of population of ASD are compared with alternate connections of individuals affected with ASD and patients with diverse genetic infections. The ecological factors are also considered as the root cause for ASD development. Prenatal exposures, aged parenting, longer gap between births, and birth complexities were embedded with ASD formation. While identifying the environmental and genetic infections to ASD, it is not replicated well and no single factor was examined in ASD. Additionally, the presentation and etiology, patients with ASD show different reactions for various treatments. A well-known treatment for ASD is Applied Behavior Analysis (ABA).

The principle behind ABA module is learning and motivation to change the timid behavior (enforces skill acquisition, limit the complicated behaviors) [5]. ABA is initialized at an earlier age and expressed on higher intensity like 25 to 40 h per week for massive days. Even though ABA shows an efficient result for ASD, the treatment response differs from each individual. Numerous factors are utilized in predicting the favorable response. The treatment aspects like treatment intensity consider a concerned number of variance monitored in treatment response, child based factors were found. Younger age, low severity of ASD signs, good IQ, robust adaptive skills, better language skills, and social skills were also related with supreme results. In spite of the reliable findings, the capability in predicting individual treatment response has been mitigated limited.

Recently, the developers have concentrated in different heuristics and statistical methodologies to comprehend and examine the models for diagnosing and recover from ASD. In this model, Machine Learning (ML) is one of the effective approaches used for examining the tedious concepts [6]. Thus, ML method is applied for implementing binomial classification tasks to find the features for predicting the infection. Only few works have concentrated on autism detection research. In particular, diagnosing ASD [7] is performed with the help of ML models where it enhances the diagnosing efficiency, for instance, [8] reduced the actual Autism Diagnostic Observation Schedule (ADOS) for massive number of behavioral parameters which has exhibited better sensitivity and specificity by mapping the performance level of developed ADOS models. In this method, Support Vector Machines (SVM) classifier has been used for ASD

Received: 16 Dec 2020
Accepted: 24 Feb 2021
Published: 27 Feb 2021

***Corresponding Author**
Email:
umasundar216@gmail.com

IIOAB JOURNAL
ISSN: 0976-3104

prediction by examining the subset of behavioral attributes in ADOS. To relate the analysis of these methods were examined using areas under ROC curves (AUCs) from the accomplished predictions on limited subset and previous subsets are projected by ADOS framework. On dividing the data as subgroups, an effective accuracy has been gained from the above-mentioned approaches.

[9] deployed a ML-centric estimation of autism with 3 complementary approaches for providing a diagnostic and better result: The 4-minute long, parent-report study has been accomplished by mobile apps, collection of basic behavioral parameters obtained from arbitrary clips of children, and a 2-minute study acquired from the physician in medical estimation. As a result, better medical analysis has been accomplished in US, over the age of 18–72 months. [10] projected a novel mobile application which has been applied for resolving the complexity in customers and health research community a friendly, time-effective, and applicable mobile-oriented ASD screening named as ASD Tests. [11] introduced an effective prediction approach according to ML model for developing a mobile application for ASD forecasting. It is manufactured under the combination of Random Forest CART and RF-ID3. The methods were computed with AQ-10 dataset, and real-time datasets have been gathered from users affected with autistic defects. Therefore, performance estimation has showcased that the presented approach has gained better accuracy for children, maximum in adolescents and greater in adults with AQ-10 datasets with optimal accuracy than real datasets.

This paper presents a new ASD diagnosis model using quasi oppositional-based dragonfly algorithm (DOA) for feature selection (QODF) with deep SAE network (DSAN). The proposed QODF-DSAN model incorporates quasi oppositional based learning (QOBL) concept to increase the convergence rate of DOA. The QODF algorithm is employed for selecting an optimal subset of features. In addition, the DSAN model is applied for classification purposes. To ensure the effective performance of the QODF-DSAN model, a set of simulations occur on three benchmark dataset.

METHODS

In overall working process of the QODF-DSAN method is shown in [Fig. 1]. As depicted, a patient's medical data is primarily preprocessed to improve data quality. After that, QODF algorithm is applied to select an optimal set of features. At last, the feature reduced subset is fed into the DSAN based classifier to determine the appropriate class labels.

Preprocessing

Initially, patient data is preprocessed in 3 stages namely format conversion, missing value replacement, and class labeling. At first, the input data in .arff format is changed into the companionable .csv format. Also, the missing values take place in the dataset are occupied by the median method. Finally, the class labeling process is carried out to map the class labels of the data into ASD.

Feature Selection Process using QODF algorithm

Once the patient data is preprocessed, QODF algorithm is executed to choose an optimal set of features. The QOBL is included to the DF algorithm to increase the convergence rate.

In dragonfly Algorithm (DA) is a recently developed bio-inspired optimization method deployed by [12]. It is mainly evolved from dynamic and static performances of dragonflies swarming behavior. Dragonflies are generally the class of fancy insects. Around 3000 varieties of these insects were found globally. Specifically, Nymph and adult are 2 major phases of dragonfly's lifecycle. Thus, nymph stage is passed for many years and then enters into metamorphism stage. Dragonflies are tiny predators. Additionally, nymph dragonflies consume tiny fishes and alternate types of marine insects. The DA approach is composed of 2 objectives namely, Hunting (static swarm) and Migration (dynamic swarm). In case of static swarm, dragonflies make tiny groups and move backward within a designated region for hunting the flying victims. A flying way feature of static swarm is immediate changes and local movements. Therefore, the feature differs from dynamic swarm, as larger dragonflies, count of migrating over longer distances create the swarm to move in single direction. It is evolved from developing sub-swarms and flies over numerous areas in a dynamic swarm that aims in exploration phase whereas static swarm tries to move in bigger swarms as decided in exploitation phase [13].

In DA model, 3 primitive strategies of swarming behavior are defined in the following:

- Separation: It means the elimination of individuals' static collision from each other.
- Alignment: It means the individual velocity corresponding to alternate neighbourhood separates.
- Cohesion: it refers individuals' capacity to neighborhood' mass center.

IIOAB JOURNAL
ISSN: 0976-3104

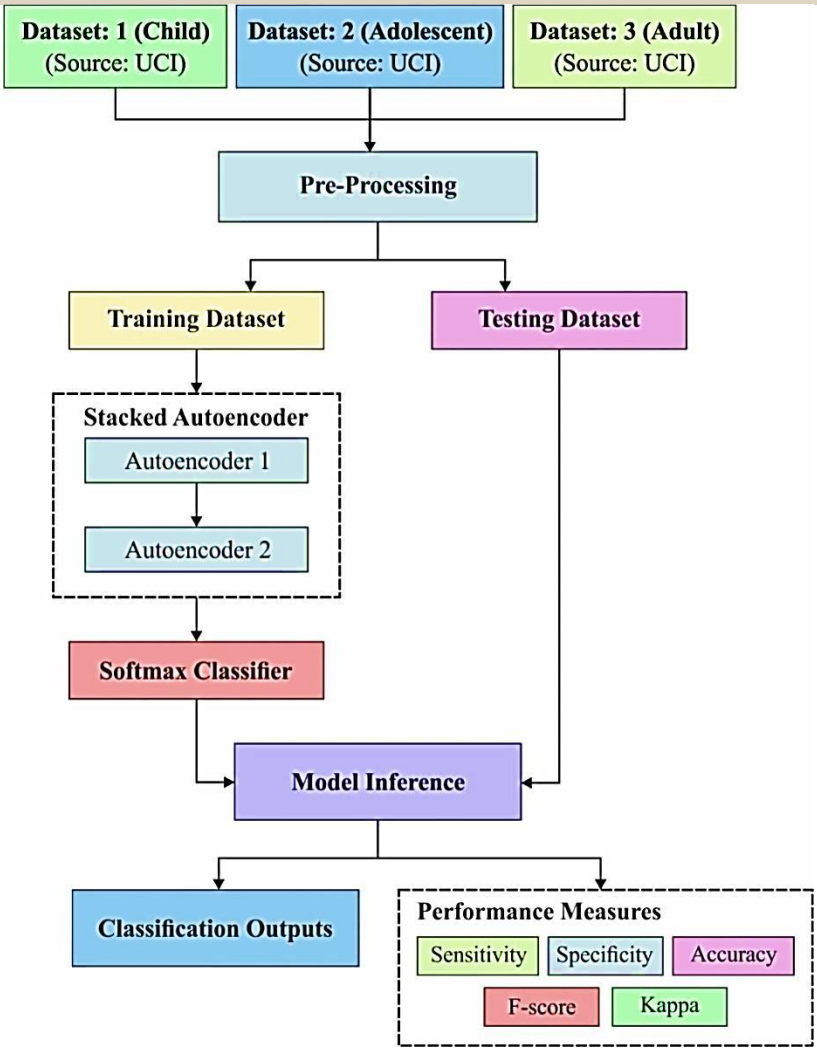

Fig. 1: Overall process of QODF-DSAN model.

Survival rate is one of the major goals of any swarm where each individual is disturbed externally and attracted to the food direction. Because of this behavior, 5 important attributes affect the individuals' upgrading location are Separation, Alignment, Cohesion, Attraction towards food source, and Distraction of enemy. Such attributes are explained numerically as given below.

Separation: This parameter is measured by given formula:

$$S_i = -\sum_{k=1}^{M} Y - Y_k, \tag{1}$$

where Ymeans the individual's recent place, Y_k denotes the location of *k-th* neighboring individual and Mdefines the overall count of neighboring separations.

Alignment: It shows the mean of velocities which is determined by given expression:

$$A_i = \frac{\sum_{k=1}^{M} V_k}{M}, \tag{2}$$

where $V_k$implies the velocity of *k-th* neighboring individuals.

Cohesion: In this attribute is evaluated as follows:

$$C_i = \frac{\sum_{k=1}^{M} Y_k}{M} - Y \tag{3}$$

Attraction towards a food source: It signifies a distance among location of present individual and location of food source (Y^+) and it can be determined by the provided notion:

IIOAB JOURNAL
ISSN: 0976-3104

$$F_i = Y^+ - Y \tag{4}$$

Distraction outwards an enemy: It means a distance among position of recent individual and location of an enemy (Y^-) which is measured by:

$$E_i = Y^- - Y \tag{5}$$

In dragonfly, nature is a unification of 5 variables. Then, 2 vectors are employed for upgrading dragonflies' place in a search space, such as step vector ($\triangle Y$) and position vector (Y). Step vector is illustrated by the given function:

$$\triangle Y_{t+1} = (aA_i + sS_i + cC_i + eE_i + fF_i) + w \triangle Y_t\,, \tag{6}$$

where a means the alignment weight, $A_i$refers to the alignment of *i-th* individual, $s$denotes the separation weight, $S_i$implies the differentiation of *i-th* individual, $c$defines the cohesion weight, $C_i$represents the cohesion of *i-th* individual, e depicts enemy weight, $E_i$defines the location of enemy in *i-th* individual, $f$signifies the food weight, $F_i$showcases a food source of *i-th* individual, w shows the inertia weight, and t exhibits the described as iteration number.

The individual's position vector is depicted as given in the following:

$$Y_{t+1} = Y_t + \triangle Y_{t+1} \tag{7}$$

In case of optimization mechanism, diverse exploitative and explorative behaviors have been accomplished by using 3 variables (a, s, c, e, and f). Besides, these parameters are also employed in managing exploration and exploitation phases.

In dragonflies' convergence is ensured by the iterations of parameters weight that is modified accordingly. Hence, flying direction of dragonflies was changed as an optimization model is processed.

This approach utilizes a random walk (Lèvy flight) for improvising stochastic, randomness as well as DA searching. An upgrading location of dragonflies is described as given in the following:

$$Y_{t+1} = Y_t + \text{Lèvy}(d) \times Y_t, \tag{8}$$

$$Lèvy\,(y) = 0.01 \times \frac{n1 \times \sigma}{|n_2|^{\frac{1}{\beta}}},$$

$$\sigma = \left(\frac{\Gamma(1+\beta) \times sin\left(\frac{\pi\beta}{2}\right)}{\Gamma\left(\frac{1+\beta}{2}\right) \times \beta \times 2^{\left(\frac{\beta-1}{2}\right)}} \right)^{1/\beta}$$

where d shows the dimension of position vector, $n1$, $n2$ means 2 random valued in $[0, 1], \beta$ implies a constant, and $\Gamma(x) = (x-1)$!. To enhance the convergence rate of DF technique, QOBL concept is introduced.

Initially, OBL is coined by Tizhoosh [14] which ensures the efficient model for particle swarm optimization (PSO), differential evolution (DE), and ant colony optimization (ACO). Similar to Evolutionary Algorithms (EA), biogeography-based optimization (BBO) is invoked as population string that has been produced randomly if there is no primary knowledge regarding the known solution space. Hence, process of evolution is terminated once reaching the stopping criteria. The processing time is directly proportional to distance of guess from best result. The possibilities of accomplishing best results are enhanced by initializing closer (fittest) solutions by validating the inverse solution at the same time.

QODF algorithm for FS

Feature Selection (FS) is referred as a binary optimization issue, in which solutions are limited to binary {0, 1} values. Thus, binary extension of DA model is applicable for resolving the above-mentioned problem. Here, vector of 0s and 1s have been executed to exhibit the accurate solution for a given problem, where the 0 refers the equivalent feature is not decided while 1 represents the required feature is decided. During this approach, a wrapper FS model which depends upon DA method has been presented. Followed by, DSAN classification approach has been employed to estimate the decided feature subsets. FS is assumed as multi-objective issues in which 2 contradictory objectives should be accomplished to enhance the classification accuracy and try to mitigate the count of decided features. Thus, cardinality of reduct is applied in the objective function and classification error rate. Eq. (9) implies the objective function.

IIOAB JOURNAL
ISSN: 0976-3104

$$Fitness = \alpha\gamma_R(D) + \beta\frac{|R|}{|c|} \quad (9)$$

where $\gamma_R(D)$ denotes the classification error rate of DSAN classifier. Moreover, $|R|$ refers the cardinality of chosen subset and $|C|$ means the overall count of features in a dataset, α, and β are 2 attributes that shows the significance of classifier quality as well as subset length, $\alpha \in [0, 1]$ and $\beta = (1\text{-}\alpha)$ applied s from [15].

DSAN based Classification

At the last stage, the feature reduced subset is given as input to the DSAN model, which executes the classification process to find out the proper class labels. Generally, Autoencoder (AE) is evolved from Deep Learning (DL) structure which is same as Artificial Neural Network (ANN) applied to perform encoding and decoding operations for input as relied on unsupervised learning. In easy AE system which is embedded with input, hidden, and resultant layer as same as ANN. Every layer in ANN contains certain number of neurons. Input and resultant layers are composed of identical count of neurons whereas hidden layer is composed of minimum neurons that make an effective process than feed-forward neural networks (FFNN).

Initially, an input is supplied to AE and considers it as x. Followed by, the input vector is encoding to accomplish hidden code by applying encoder portion that is provided as input to decoding portion. Hence, decoder portion is responsible for reforming original input from code, x'.

The central premises of AE are to filter essential featured by limiting the data size and for obtaining noise-free information. Eq. (10) is applied in encoding phase to accomplish code c while Eq. (11) is employed in decoder phase to recreate the input data x. Next, BackPropagation (BP) method is utilized for calculating the error as provided in Eq. (12) that is used for fine-tuning the system and to make their formed output as adjacent to input data. Hence, basic idea of developed approach is to mine significant designs in the applied data.

$$c = F(w^t x + b) \quad (10)$$

$$x' = F(wc + b') \quad (11)$$

$$e = \min \sum_{i=1}^{n} (x' - x)^2 \quad (12)$$

In Eq. (10) and (11), Frefers the activation functions applied, b implies the bias value and w signifies the weights of input and hidden layer. The value x' exhibits the reformed form of input $x$by applying c. The regularization is employed to mitigate the over-fitting in ANN as depicted in Eq. (13).

$$\min \left[\left\{ \sum_{i=1}^{n} (x' - x)^2 \right\} + \gamma L(w) \right] \quad (13)$$

In Eq. (13), L(w) refers the weight alteration variable while γimplies the regularization term. These values are selected using hit and trial method. Several AEs are "stacked" in greedy layer-wise fashion for invoking the weights of Deep Neural Network (DNN) to accomplish a deep-stacked AE.

Next, these features are induced as a softmax classifier to classified issues. A softmax layer is employed behind DSAN to classify the input data. It applies the essential features and guides in enhancing the classification function.

$$F(x_i) = \frac{Exp(x_i)}{\sum_{j=0}^{k} E\,xp(x_j)}, where\ i = 0, 1, \cdots, k \quad (14)$$

The Eq. (14) signifies the softmax function. It determines the exponential of given input x_i and the summation of exponential values and fractions result in softmax function [16]. For multi-classification module, softmax function offers the possibilities of every class in which output class should have maximum probability when compared with all other classes.

RESULTS AND DISCUSSION

In productive classification results of the QODF-DSAN method has been sampled over 3 ASD dataset. The ASD children, Adolescent, and Adult dataset [17-19] are composed of 292, 104, and 704 sampled with same set of 21 features.

Table 1 signifies the FS outcomes of the QODF-FS scheme with traditional approaches by means of optimal cost and selected set of features. The table refers that the PCA-FS approach is considered a poor

IIOAB JOURNAL
ISSN: 0976-3104

FS approach, which has gained low best cost of 0.9208. Simultaneously, the GA-FS and PSO-FS methodologies have gained moderate best cost of 0.8167 and 0.7891 correspondingly. Similarly, the GWO-FS framework has attained closer optimal results with a maximum cost of 0.6523. Meantime, the QODF-FS scheme has depicted supreme results with a best cost of 0.3127.

Table 1: Selected Features of Existing with Proposed QODF-FS Method

Methods	Best Cost	Selected Features
QODF-FS	0.3127	1,2,3,4,7,9,10,11,14,15,20
GWO-FS	0.6523	1,4,5,6,7,8,9,11,12,13,14,15,16,17,19
PSO-FS	0.7891	3,4,5,6,7,8,10,11,12,13,14,15,16,17,18
GA-FS	0.8167	1,5,6,7,9,10,12,13,15,16,17,18,19,20
PCA-FS	0.9208	2,4,5,6,7,8,9,10,11,12,13,14,15,16,17,18,19

Table 2 depicts a brief comparative results analysis of the QODF-DSAN method with traditional approaches [20-22] by means of diverse metrics. On measuring the classifier outcome by means of accuracy, the worse classifier performance is illustrated by DT with the minimum accuracy of 54.7%.

Table 2: Result Analysis of Existing with Proposed QODF-DSAN Method on Applied Dataset

Methods	Sensitivity	Specificity	Accuracy	F-score	Kappa
QODF-DSAN(Children)	97.86	97.37	97.60	97.51	95.19
QODF-DSAN(Adolescent)	95.31	98.83	97.87	96.06	94.60
QODF-DSAN(Adult)	96.88	97.50	97.12	97.64	93.93
Decision tree	53.30	54.90	54.70	-	-
Logistic regression	55.50	62.60	59.10	-	-
Neural network	53.30	71.20	62.00	-	-
k-Nearest neighbor	46.60	72.10	61.80	-	-
SVM (linear)	57.10	66.70	61.40	-	-
RF-CART	82.06	77.02	80.71	-	-
Optimal-KNN	-	-	69.20	-	-
Optimal-LR	-	-	68.60	-	-
Optimal-RF	-	-	67.78	-	-

Then, the LR model has surpassed the DT with the moderate accuracy of 59.1%. Moreover, the SVM (linear), KNN, and NN methodologies have attained acceptable classification results with a closer accuracy of 61.4%, 61.8%, and 62%. Afterward, the Optimal-RF, Optimal-LR, and Optimal-KNN frameworks have illustrated considerable accuracy values of 67.78%, 68.6%, and 69.2%. Even though the RF-CART scheme has performed well than classical methods with an accuracy of 80.71%, it is ineffective to represent better outcomes over the projected QODF-DSAN model which has gained optimal accuracy of 97.6%, 97.87%, and 97.12% on ASD-Children, ASD-Adolescent, and ASD-Adult dataset correspondingly.

On determining the classifier outcomes interms of sensitivity, the inferior classifier function is depicted by kNN with minimum sensitivity of 46.6%. Then, the NN and DT models have outperformed the kNN with acceptable and closer sensitivity of 53.3%. Moreover, the LR approach has achieved considerable classification outcomes with sensitivity of 55.5%. Followed by, the SVM (linear) scheme has exhibited moderate sensitivity value of 57.10. Though the RF-CART model has surpassed the previous approaches with the sensitivity of 82.06%, it has failed to exhibit better results over the presented QODF-DSAN approach which has accomplished higher sensitivity of 97.86%, 95.31%, and 96.88% on ASD-Children, ASD-Adolescent, and ASD-Adult dataset respectively. From the detailed experimental analysis, the resultant simulation outcome verified the effective classification results with the higher accuracy of 97.60%, 97.87%, and 97.12% on ASD-Children, ASD-Adolescent, and ASD-Adult dataset respectively.

CONCLUSION

This paper has presented a new ASD diagnosis method utilizing QODF-DSAN model. The processes involved in the ASD diagnosis are preprocessing, FS, and classification. The patient's medical data is primarily preprocessed to improve the data quality. After that, QODF algorithm is applied to select an optimal set of features. At last, the feature reduced subset is fed into the DSAN based classifier to determine the appropriate class labels. To ensure the efficient performance of the QODF-DSAN method, a set of simulations takes place on three benchmark datasets. The resultant simulation outcome verified the effective classification results with a higher accuracy of 97.60%, 97.87%, and 97.12% on ASD-Children, ASD-Adolescent, and ASD-Adult dataset respectively. In future, the proposed model can be implemented in real time to assist physicians in ASD diagnosis.

CONFLICT OF INTEREST

There is no conflict of interest.

ACKNOWLEDGEMENTS
None

FINANCIAL DISCLOSURE
None.

REFERENCES

[1] DSM-IV-TR. AP. [2000] Diagnostic and statistical manual of mental disorders. Washington, DC: American Psychiatric Association.
[2] Lord C, Petkova E, Hus V, Gan W, Lu F, Martin DM, Ousley O, Guy L, Bernier R, Gerdts J, Algermissen M. [2012] A multisite study of the clinical diagnosis of different autism spectrum disorders. Archives of general psychiatry. 5;69(3):306-13.
[3] Grzadzinski R, Huerta M, Lord C. [2013] DSM-5 and autism spectrum disorders (ASDs): an opportunity for identifying ASD subtypes. Molecular autism. 4(1):1-6.
[4] Kanne SM, Gerber AJ, Quirmbach LM, Sparrow SS, Cicchetti DV, Saulnier CA. [2011] The role of adaptive behavior in autism spectrum disorders: Implications for functional outcome. Journal of autism and developmental disorders. 41(8):1007-18.
[5] Granpeesheh D, Tarbox J, Dixon DR. [2009] Applied behavior analytic interventions for children with autism: a description and review of treatment research. Annals of clinical psychiatry. 21(3):162-73
[6] Wall DP, Kosmicki J, Deluca TF, Harstad E, Fusaro VA. [2012] Use of machine learning to shorten observation-based screening and diagnosis of autism. Translational psychiatry. 2(4):e100-.
[7] Du Y, Fu Z, Calhoun VD. [2018] Classification and prediction of brain disorders using functional connectivity: promising but challenging. Frontiers in neuroscience. 12:525.
[8] Küpper C, Stroth S, Wolff N, Hauck F, Kliewer N, Schad-Hansjosten T, Kamp-Becker I, Poustka L, Roessner V, Schultebraucks K, Roepke S. [2020] Identifying predictive features of autism spectrum disorders in a clinical sample of adolescents and adults using machine learning. Scientific reports. 10(1):1-1.
[9] Abbas H, Garberson F, Liu-Mayo S, Glover E, Wall DP. [2020] Multi-modular AI approach to streamline autism diagnosis in young children. Scientific reports. 10(1):1-8.
[10] Thabtah F. [2019] An accessible and efficient autism screening method for behavioural data and predictive analyses. Health informatics journal. 25(4):1739-55.
[11] Omar KS, Mondal P, Khan NS, Rizvi MR, Islam MN. [2019] A machine learning approach to predict autism spectrum disorder. In2019 International Conference on Electrical, Computer and Communication Engineering (ECCE). 1-6.
[12] Mirjalili S. [2016] Dragonfly algorithm: a new meta-heuristic optimization technique for solving single-objective, discrete, and multi-objective problems. Neural Computing and Applications. 27(4):1053-73.
[13] Sayed GI, Tharwat A, Hassanien AE. [2019] Chaotic dragonfly algorithm: an improved metaheuristic algorithm for feature selection. Applied Intelligence. 49(1):188-205.
[14] Tizhoosh HR. [2005] Opposition-based learning: a new scheme for machine intelligence. International conference on computational intelligence for modelling, control and automation and international conference on intelligent agents, web technologies and internet commerce (CIMCA-IAWTIC'06). 1:695-701.
[15] Mafarja MM, Eleyan D, Jaber I, Hammouri A, Mirjalili S. [2017] Binary dragonfly algorithm for feature selection. In2017 international conference on new trends in computing sciences (ICTCS). 12-17.
[16] Khamparia A, Saini G, Pandey B, Tiwari S, Gupta D, Khanna A. [2019] KDSAE: Chronic kidney disease classification with multimedia data learning using deep stacked autoencoder network. Multimedia Tools and Applications.1-6.
[17] https://archive.ics.uci.edu/ml/datasets/Autistic+Spectrum+Disorder+Screening+Data+for+Children++
[18] https://archive.ics.uci.edu/ml/datasets/Autistic+Spectrum+Disorder+Screening+Data+for+Adolescent+++
[19] https://archive.ics.uci.edu/ml/datasets/Autism+Screening+Adult
[20] Parikh MN, Li H, He L. [2019] Enhancing diagnosis of autism with optimized machine learning models and personal characteristic data. Frontiers in computational neuroscience. 13:9.
[21] Omar KS, Mondal P, Khan NS, Rizvi MR, Islam MN. [2019] A machine learning approach to predict autism spectrum disorder. In2019 International Conference on Electrical, Computer and Communication Engineering (ECCE). 1-6.
[22] Devika Varshini G, Chinnaiyan R. [2020] Optimized Machine Learning Classification Approaches for Prediction of Autism Spectrum Disorder. Ann Autism Dev Disord. 1(1).;1001.

IIOAB JOURNAL

ARTICLE

CONTRIBUTION OF ENERGY STORAGE IN IMPROVING THE INTEGRATION OF GRID-TIED PHOTOVOLTAIC SYSTEMS

Badr Alshammari[1], Rabeh Abbassi[1,2*], Abdelkader Abbassi[3], Salem Saidi[4], Awad S. Alashammari[1], Khalid Alqunun[1], Tawfik Guesmi[1]

[1]Department of Electrical Engineering, College of Engineering, University of Hail, KINGDOM OF SAUDI ARABIA
[2]Department of Electrical Engineering, ENSIT, LaTICE Lab., University of Tunis, TUNISIA
[3]Department of Electrical Engineering, ENSIT, LISIER Lab., University of Tunis, TUNISIA
[4]Department of Electronic Engineering, National Institute of Advanced Technologies of Borj Cedria, University of Carthage, TUNISIA

ABSTRACT

With the increased use of PV systems (PVSs) and the growth of their penetration level in the modern power systems, the effectiveness of grid-tied PV systems have become a spotlight topic for researchers in this field. As a contribution in the efforts aiming to improve the effectiveness of the PV systems integration to the electric grid, the objective of this paper is to investigate the performance of a grid-connected PV system that uses a bank of storage batteries. The battery storage system is integrated via a reversible chopper to perform the role of a buffer between the PVS and the point of coupling with the grid. A control method based on an optimal energy management approach (EMA) has been established to control the involved DC-DC and DC-AC converters. Furthermore, the contribution of the storage system has been discussed. Indeed, two study scenarios without and with the contribution of the storage system were considered and analyzed. Simulations under Matlab/Simulink® have been carried out to prove the performance of the proposed control method and the adopted power flow management. The found results prove the efficiency of the developed control strategy to ensure the connection of the hybrid system to the grid, while guaranteeing the power quality requirements.

KEY WORDS
Photovoltaic Systems; Storage Battery; Power quality; DC bus voltage regulation; Energy management

Received: 9 Nov 2020
Accepted: 10 Feb 2021
Published: 3 Mar 2021

***Corresponding Author**
Email:
r.abbassi@uoh.edu.sa

INTRODUCTION

During last decades, fuel consumption and CO_2 emission increased due to the use of conventional power plants [1]. Serious attempts have been made to increase the energy self-sufficiency and meet CO_2 emission reduction target for both developed and in development countries [2], [3]. In this context, renewable energy sources have been included to ensure the energy security, the environmental sustainability and to play an essential role in future mix of energy policy [4]. Driven by relevant incentive policies, the grid-connected photovoltaic systems have been expanded widely due to the decreasing trend of capacity cost [5]. Thereby, PV energy harvesting systems have become the fastest growing renewable technology.

Grid-connected PV power systems can increase the proportion of solar energy on the power grid to reduce pollutant emissions, especially greenhouse gas (GHG) emissions, and global warming [6].

The major problems of PVGs are mainly around the following four levels [7-10]:

- The level of generation and the duty to extract, at any time, the maximum power available through the operation of commands based on techniques (MPPT) driving the DC-DC converters.
- The level of the DC-AC converter used to convert the direct current produced by the photovoltaic panels into alternating current adapted to the electrical network. Such an inverter plays a crucial role in solar energy production installations as it serves as a bridge between the photovoltaic system and the electricity grid, whether for a residential installation or a power plant.
- The level of synchronization and integration of photovoltaic and fluctuating energy in the electrical network.
- The level of the obligation to use a battery storage system in order to continuously ensure the availability of energy and to meet the demand for power demanded by the load.

By reason of the intermittent behavior of solar irradiation in nature, which is generally unpredictable, the production of energy from PV introduces more uncertainty in the operation of an autonomous microgrid integrating these generators [11]. The main challenge of using the sun as an energy source is that it may not be available when electricity is needed. Therefore, the incorporation of the energy storage system (ESS) allows the reduction of the uncertainty of the solar production is essential to improve the reliability and security of production. The ESS can play a key role in the energy generation and thus smoothing of the fluctuations in produced solar energy over a desired time horizon [12]. The ESS can also be used to offset the variations in load power.

Although the use of energy storage combined with a grid-connected PV system is still recent, there are already numerous configurations of integration of battery storage in solar generators. These configurations vary primarily based on functionality and application. The most distinctive topologies are AC voltage side

IIOAB JOURNAL
ISSN: 0976-3104

coupling (AC systems) and DC voltage side coupling (DC systems) [13]. It is obvious that each of these topologies and its sub-variants has its particular advantages and disadvantages.

For the AC side coupling, the battery is coupled to the grid via an inverter. In general, this allows the storage system to be recharged from the grid other than the reinjection into the home network [14]. For this topology, the battery is installed and used independently of the PV system. If needed, these systems can also recharge the battery from the grid and not just from the PVS. Such systems may also be installed in homes where the PV system already exists but does not yet have storage or in case of extension of an existing storage system. This topology has some advantages namely the possibility of retrofitting an existing PV system, more flexibility and choice in the size of the systems and the modular possibility to increase it. Otherwise, its disadvantages revolve around the need for more space, the higher price because of the redundancy of the inverters (2 inverters required) and, in certain situations, the complexity of the calculating.

For the DC side coupling, the battery only stores solar energy while solar inverters are solely responsible for powering the grid. Some new photovoltaic inverters have been designed to also function as battery chargers. In this situation, the battery is charged by the DC side of the inverter. The connection of the PV-Battery system to the mains is ensured via the same inverter. Fewer elements are needed for the same functionality, which often gives cost and space advantages. In addition, the current generated by the PV system undergoes fewer conversion steps to the battery. In use, conversion losses are thus typically smaller. However, the actual losses will largely depend on the efficiency of the installed equipment. There is often a device to charge the battery by the grid during emergency [10]. This topology has advantages related to the savings in materials, thus reducing costs and the necessary space. In addition, if the battery is not charged by the network, the counting device is identical to that of a standard solar system. The main disadvantages are mostly related to the complexity of a possible extension of the system and the loss of flexibility due to the coordination of the PV- Battery sizing. Within the framework of self-sustaining autonomous energy systems, the feasibility assessment of hydrogen and battery storage device supporting a domestic PV system has been studied in [15]. The insufficiency of this work can be summed up to the fact that the dimensioning was limited to off-grid operation. Balint et al. have conducted a deep yearly comparison between various discharge methods of residential PV-Battery systems connected to the grid [16]. Though the found results are satisfactory for manufactures' BESS in terms of facilitating different system comparisons, other issues related to hybrid systems have not been investigated.

While considering the trade-off between various factors such as the storage health and the energy cost, an optimal planning of solar systems incorporating a battery bank was presented [17]. Furthermore, Asmae et al. approached a method of energy management for serving the load when the solar-battery system is connected to the grid [18].

In what follows, the material and methods section presents the basis of the modeling and the development of numerical models to be simulated, including those of the PVG and MPPT control, the storage system and its control and the inverter control. Afterwards, the results section focuses on the presentation and the discussion of the results of the developed simulations, dealing in particular with two scenarios i.e. without and with storage system. Finally, the conclusions and the future trends are given.

MATERIALS AND METHODS

The topology of the studied three-phase grid-connected PV system is illustrated in Figure 1. The scheme is based on a DC/DC boost converter which is in charge of both the MPP tracking of the PV generator and the generated power curtailment during grid voltage unbalances [19, 20]. In addition, a 2-level three-phase dc/ac stage ensures the connection to the grid via a LCL filter. The inverter is in charge of controlling the dc-link voltage control and the injecting of the generated power into the grid. Otherwise, the LCL filter is exploited to decrease the attenuation of the harmonics caused by the switching [20, 21].

This section focuses on the modeling and control of the whole system under study. Indeed, a first part was reserved for the modeling of the PV generator and the control of its step-up chopper via MPPT algorithm. A second part was focused on the study of the storage system and the control technique of the reversible chopper responsible for charging and discharging the battery bank. In addition, the third part was given to the control of the AC-AC converter on the grid side.

PVG Modelling and MPPT control

It is important to note that the modeling of the PVG was made by adopting the circuit with two diodes thanks to its accuracy compared to the model with two diodes [22]. By neglecting the characteristic resistances, the generated current is expressed as follows.

$$i_{PV}(G,T) = \frac{G}{G_n}\left[I_{scn} + K_i(T - T_n)\right] - \frac{I_{scn} + K_i(T - T_n)}{\exp\left(\frac{V_{ocn} + I_{scn}(T - T_n)}{nN_s k_B T/q}\right) - 1} \cdot \left[\exp\left(\frac{V_{PV}}{nN_s k_B T/q}\right) - 1\right] \quad (1)$$

IIOAB JOURNAL
ISSN: 0976-3104

where N_s is the number of PV cells connected in series to form the PV panel. T and G are the ambient temperature and irradiation, respectively. T_n and G_n are the temperature and irradiation at standard test conditions (STC), respectively. q is the charge of an electron, k_B is Boltzmann constant, n is the diode ideality factor. V_{ocn} and I_{scn} are the open circuit voltage (V_{oc}) and the cell's short circuit current (I_{sc}) at STC and k_v and k_i are the variation coefficients of the V_{oc} and the I_{sc}, respectively.

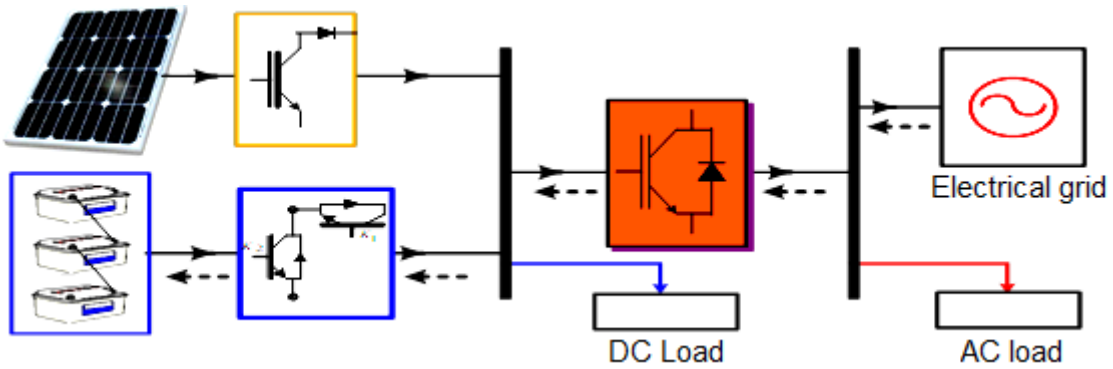

Fig. 1: Grid-connected PV-Battery hybrid system.

To simulate the current and voltage, and therefore the power, of the PV generator containing N_{ss} panels associated in series and N_p panels connected in parallel, Eq. (1) is rewritten as in Eq. (2) and the power as in Eq. (3):

$$i_{pv}(G,T) = \frac{G}{G_n} N_p [I_{scn} + K_i(T - T_n)] - \frac{(I_{scn} + K_i(T-T_n))N_p}{\exp\left(\frac{(V_{ocn} + I_{scn}(T-T_n))N_{ss}}{nN_sN_{ss}k_BT/q}\right) - 1} \cdot \left[\exp\left(\frac{v_{PV}}{nN_sN_{ss}k_BT/q}\right) - 1\right] \quad (2)$$

$$P_{pv}(G,T) = i_{pv}(G,T).\, v_{pv}(G,T) \quad (3)$$

In order to locate the MPP, it is essential to express the power derivative with regard to the generator voltage to obtain the following new characteristic function:

$$P_{pv}(G,T,v_{pv}) = \left\{ \frac{G}{G_n} N_p [I_{scn} + K_i(T - T_n)] - \frac{(I_{scn} + K_i(T-T_n))N_p}{\exp\left(\frac{(V_{ocn} + I_{scn}(T-T_n))N_{ss}}{nN_sN_{ss}k_BT/q}\right) - 1} \cdot \left[\exp\left(\frac{v_{PV}}{nN_sN_{ss}k_BT/q}\right) - 1\right] \right\} \times v_{pv}(G,T) \quad (4)$$

With a view to identify the combination of temperature and irradiance allowing to extract the maximum power point tracking (MPPT) via incremental conductance (IC) MPPT technique, the power derivative is calculated. After determining the voltage value which corresponds to the maximum power, the duty cycle of the PVG side DC/DC chopper is adjusted.

The MPPT controller is designed to overcome the constraints generated by climatic conditions which are constantly in continuous and even rapid changes [7]. The performance of this controller depends essentially on the robustness of this controller in the face of sudden atmospheric changes and in particular on the speed of reaching the MPP and on the way of oscillating nearby it. In this paper, an Improved Incremental Conductance (IIC) MPPT algorithm controls the PV side boost converter [5].

Storage system modelling and control

In a PV installation, the storage corresponds to the conservation of the PVG energy, waiting for later use. The management of solar energy requires considering storage according to weather conditions. In a general way, the storage of electrical energy passes through a form of intermediate energy (such as electromagnetic, kinetic, thermal, gravity, compression, electrostatic, electrochemical ...) convertible into electricity. According to the bibliography, there are two types of storage to consider: short-term storage (less than 10 minutes) and long-term storage (more than 10 minutes) [12-14]. The selection of the appropriate storage system is founded on mass power, mass energy, number of operating cycles, cost and energy efficiency.

Generally, the storage size is determined by the period of time over which the batteries are able to cover the average consumption without the participation of any other power source. When sizing a storage battery bank, limitations in both charge and in discharges rates have to be considered [5]. Knowing that the energy amount which can be drawn from a battery storage is determined by the ratio of discharge power to storage capacity. As declared above, the nominal battery storage capacity cannot directly be linked to the storage size.

IIOAB JOURNAL
ISSN: 0976-3104

In this work, the choice has been oriented towards Lithium-Ion batteries. This choice was justified by the efficiency that exceeds 95%, the extremely high energy density and the high power density of this type of battery. This is due to the lightness of the used electrolyte.

The purpose of the storage system is to ensure a production permanence whether for an electricity grid or a load and to absorb peaks of consumption to avoid energy imbalances. After having selected the appropriate storage mode, has such an application, the solicitations on the latter are not the same, and it is appropriate to adapt the sizing of the system subject to study depending on the intended purpose application. For our stationary application, the load profiles are rather energetic because of the needs and the energy availability over time. Thevenin's model of the battery is shown in Figure 2.

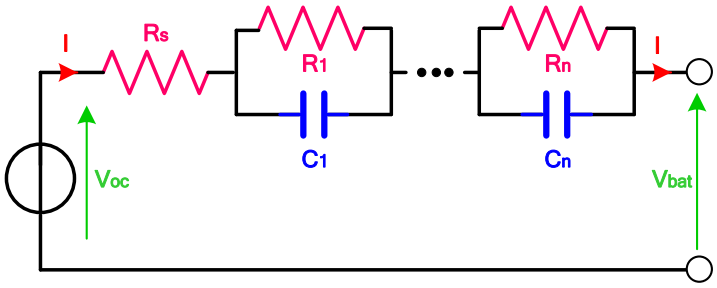

Fig. 2: N-Order battery Thevenin model.

The battery voltage V_{bat} (t) is given by:

$$V_{bat}(t) = V_{oc}(SoC(t)) - u_s(t) - \sum_{i=1}^{n} u_i(t) \quad (5)$$

$V_{oc}(SoC(t))$: Open circuit voltage changing according to the state of charge,

$u_s(t)$: Voltage drop across the terminals of Rs,

$u_i(t)$: Voltage drop across the terminals of the i^{th} *R//C* circuit.

In the literature, mainly three types of models can represent the temporal behavior of the battery: equivalent electric circuit type models, electrochemical models and black box type models (using fuzzy logic or neural networks) [13, 14]. The model that best fits our needs for the current study is shown in Figure 2. This choice was imposed by the fact that:

- the model needed aims to simulate the battery dynamic temporal behavior at low frequencies (<= 1 Hz) and the high frequency components have been neglected
- the model with *R//C* circuits can be easily applied to different batteries.
- based on Thévenin's models, the expression of each time constant (R_i, C_i) of the *R//C* circuits in series is more explicit than the transmission circuits
- the complexity of the model can be easily calibrated by modifying the number of circuits *R//C*.

In the same context, temporal characterization is chosen because:

- the temporal data are more suitable for studying the problem of relaxation with respect to frequency data.
- with the proposed structure, the battery model can be characterized only with temporal data, which avoids the use of specific equipment (impedance spectrometer).
- the battery model can be characterized even for high currents.

Given the fluctuating nature of the power generated by the PV generator, which depends primarily on meteorological conditions of irradiance and temperature, it is of utmost importance to integrate a charge regulator to block reverse charge of the PVG and protect the bank of battery against overcharging and rapid discharge. Also, the use of a bidirectional converter is imposed to ensure a secure connection of the loads of different types (DC and AC) [10]. To ensure the required efficiency and reliability, the proper choice of the converter rating is dependent on knowing the correct peak load demand on the battery and the load simultaneously.

Furthermore, it is important to note that on an industrial scale, the majority of bidirectional converters sold on the market integrate the battery charge controller.

DC-AC converter control

The mains side converter mainly deals with the conversion of direct voltage into three-phase alternating voltages. This bidirectional current inverter is made up of three switching cells, each one made up of two

IIOAB JOURNAL
ISSN: 0976-3104

IGBT transistors which are connected to two diodes in anti-parallel and controlled by PWM modulation. It is very important to mention that a DSOGI-based PLL has been adopted for the DC/DC inverter [23].

The DC / AC stage control method relies on cascade control using an internal current loop and an external voltage loop [24]. Also, the square of the DC bus voltage was controlled by a PI-based control technique according to [5]:

$$V_{dc} = \sqrt{\frac{2}{C_{dc}} \cdot \int (P_{PV} + P_{SB} - P_g^*) . dt} \quad (6)$$

RESULTS

Before presenting and discussing the simulation results, it is important to recall that many criteria have been taken into account to maximize the efficiency of the studied PV-Batteries system connected to the grid. Firstly, a great importance was paid on extracting the maximum power available from the GPV side. Indeed, in the simulated scenario, the considered sunshine and temperature profiles are those presented in figure 3 (a) and (b), respectively. Under these conditions, the optimum power generated by the PVG is depicted in figure 3 (c).

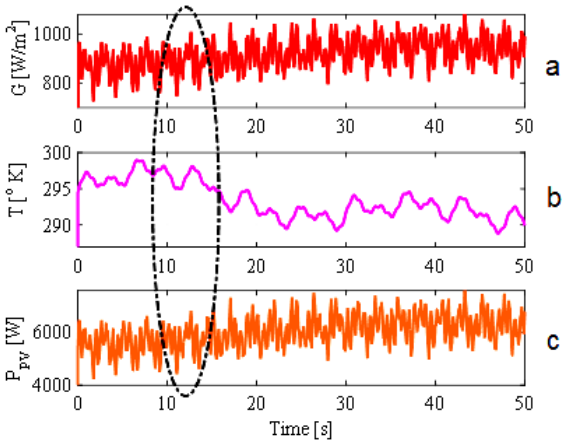

Fig. 3: Weather conditions and PVG power.

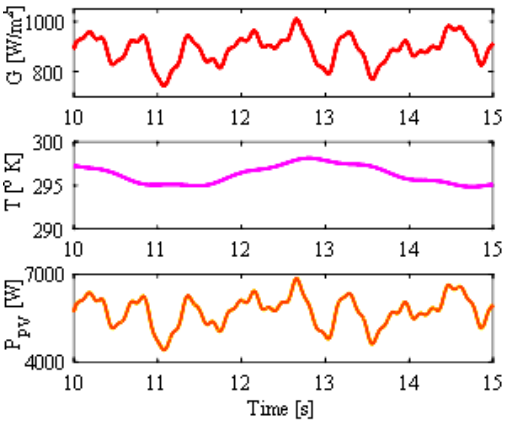

Fig. 4: Zoom version of Fig. 3.

First scenario: without storage system contribution

The first scenario consists of disconnecting the storage system. In this case all of the PVG power is injected into the PCC without the contribution of the storage system.

The power P_{PV} generated by the PVG is completely transmitted to the grid (P_g) while keeping the DC bus voltage constant. This is very clear in Figure 5 showing the shape of the power (P_g) transmitted to the point PCC and the gap between the power P_{PV} and P_g which does not exceed 15 W reflecting the losses.

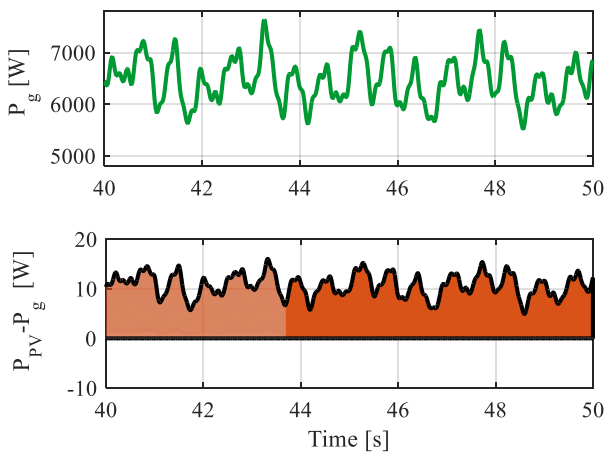

Fig. 5: Active power exchanged with the grid and power losses.

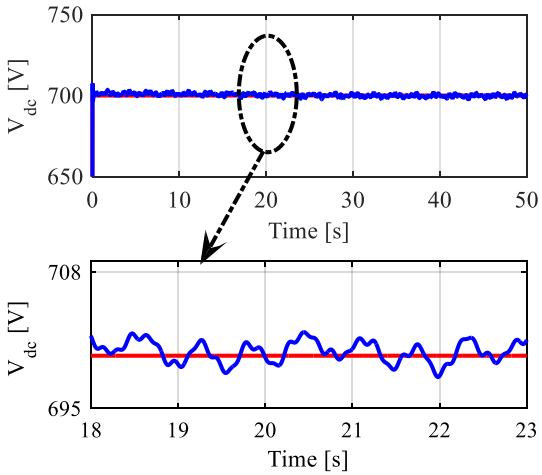

Fig. 6: DC bus voltage and its reference value.

Under the same situations, the waveform of the voltage at the DC bus level is depicted in Figure 6. It is clear that the technique of controlling the voltage of the DC bus manages to keep its value close to its reference value as depicted in the zoomed Figure 6.

IIOAB JOURNAL
ISSN: 0976-3104

With regard to the electrical quantities exchanged with the electrical network, great importance has been given to the nature of the currents injected at the PCC point and that of the voltages at the same point. The following figure (Fig. 7) shows that both the voltages are sinusoidal. Otherwise, the currents are also sinusoidal albeit their amplitude is fluctuating because it depends on the fluctuating PV generator power P_{PV} which confirms that the proposed control system is effective.

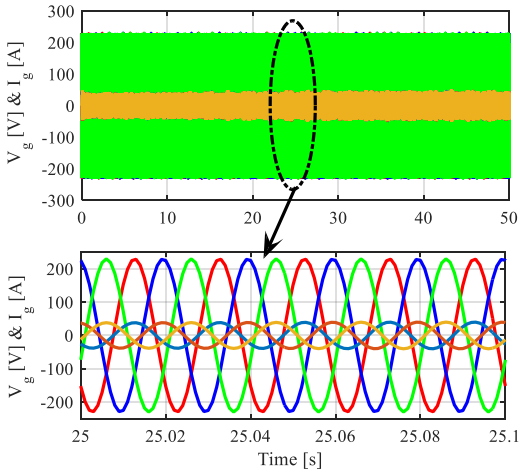

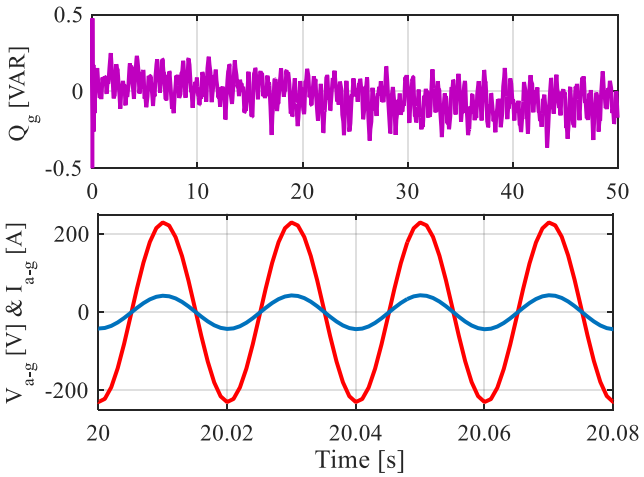

Fig. 7: Grid voltages and currents. **Fig. 8:** Reactive power and phase shift between voltages and currents at the PCC point.

Moreover, the grid reactive power is simulated in figure 8. Depending on the P_g power transmitted via the DC bus to the power grid, the reactive power is zero although negligible fluctuations are registered. In this same context, the nullity of reactive power is clearly shown by the fact that the voltage and the current of the same phase are perfectly in phase as shown in the same figure 8.

The second scenario deals with the case where the power to be injected into the network/even into the AC loads is constant (6 kW). In this case, all of the fluctuating PV power is used either to charge the storage batteries or to be fed into the PCC. This means that the storage system acts as a buffer between the PV generator and the PCC point where a constant reference grid power (P_g^*) should be maintained.

Second scenario: with storage system contribution

For this second scenario, the simulations results are also convincing. Indeed, figure 9 (a) clearly shows the success of the proposed control strategy to ensure the complementarity between the PVG and the adopted BSS and to achieve that the power injected into the grid P_g is equal to its imposed constant reference.

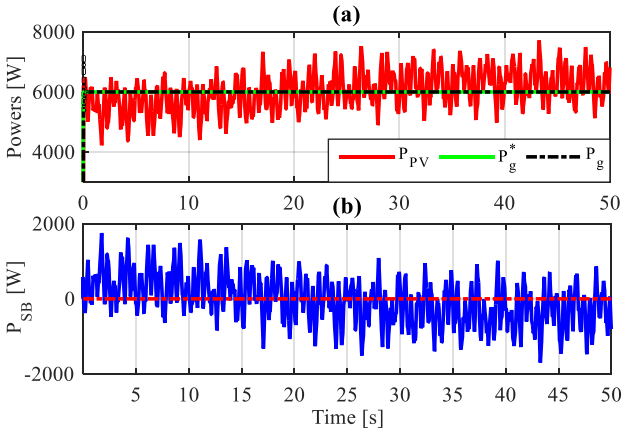

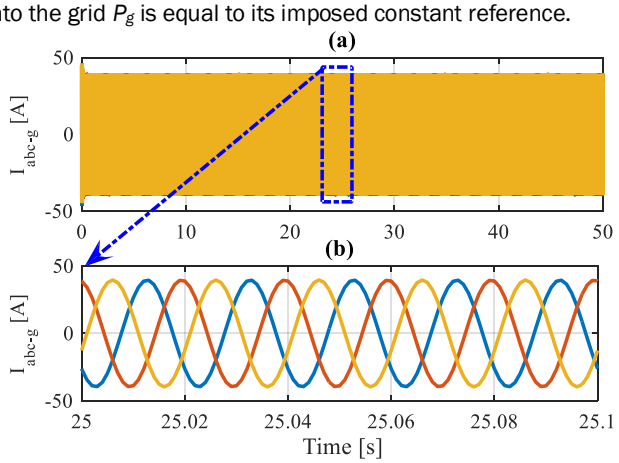

Fig. 9: Active power exchanged between the GPV, the storage system and the grid. **Fig. 10:** Grid currents waveforms.

Figure 9 (b) shows the behavior of the power exchanged between the battery storage (P_{SB}) and the DC bus. The principle of the proposed command is clearly proven. This principle consists in the fact that if the power of the GPV (P_{PV}) is greater than that of the grid (P_g), the excess is injected to charge the storage batteries. Otherwise, the lack is compensated by discharging the batteries to meet the power requirements of the PCC point (P_g^*).

IIOAB JOURNAL
ISSN: 0976-3104

Still on the grid side, the waveforms of the currents injected at the PCC point are shown in figure 10. It is clear that these currents are sinusoidal and have constant amplitude.

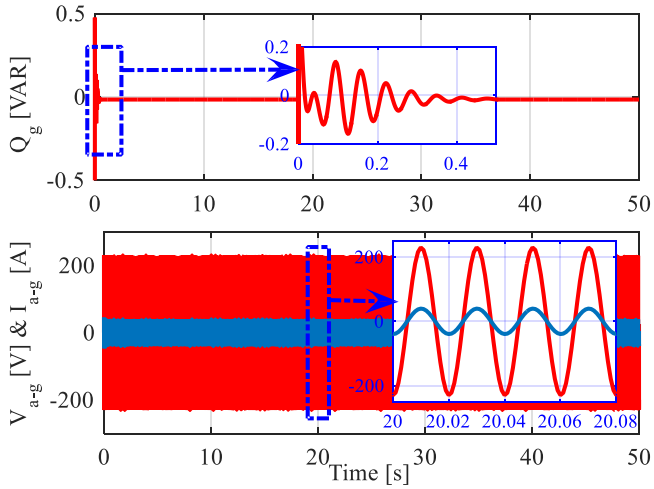

Fig. 11: Grid reactive power and grid voltage and currents.

In order to get an idea of the behavior of reactive power, figure 11 shows its zero value and its temporal evolution. Moreover, in the same figure, it is shown that the currents and voltages are in phase.
Comparative Analysis

After presenting and discussing the found simulation results, the Table 1 summarizes a brief comparative analysis. The comparative study has been based on the literature on the PV-storage systems principle. The comparison lies on the studied system configuration, its location, its On-grid or Off-grid connection, the used storage system, the type of involved battery, the main goal of the study, the adoption of an energy management approach and finally the consideration of high frequency control of power electronics converters. The conducted comparative study distinguishes the present work from the previously appeared. One can conclude that the proposed research is advantageous as it takes into account the issues of power quality and so avoids disturbing the electric grid.

Table 1: Comparative analysis

Studied System	Location	On-grid or Off-grid	Storage system	Battery type	Main objective	Energy management	High frequency converters control	Ref
Solar PV system	Finland	Off-grid	Battery + fuel cell	Lithium-ion	Technical feasibility of off-grid residential single-family house	Yes	No	[15]
Residential PV systems	Hungary	On-grid	Battery	Lithium-iron-phosphate	Comparison of different residential self-consumption-reducing discharge strategies	No	No	[16]
residential photovoltaic generation	India	On-grid	Battery	Lead acid	Increasing the profitability of a grid connected PV-Battery system	Yes	No	[17]
PV-battery residential installation	Morocco	On-grid	Battery	Not specified	Enabling the connection or the disconnection from the grid to manage its excess/lack of energy	Yes	No	[18]
PV-battery system	KSA	On-grid	Battery	Lithium-Ion	Enhancement of the PV-Battery system's ability to supply a clean and stable power flow	Yes	Yes	Our

CONCLUSIONS

This paper focuses on the piloting of a grid-connected PV system equipped with battery storage. The control system relies on different points, namely the MPPT algorithm applied to the DC/DC chopper on the

IIOAB JOURNAL
ISSN: 0976-3104

GPV side, the control of the reversible DC/DC converter controlling the charging in addition to the discharging of the battery storage system, the energy management algorithm and finally the control of the different currents and voltages of the DC/AC grid side converter to guarantee a perfect connection of the system to the PCC point. The simulations were developed using MATLAB software. The results of the simulations confirm that the presented approaches are efficient and effective for a better exploitation of the photovoltaic systems. Although the results of the simulations show satisfactory performances of the proposed method for the control of the hybrid PVG-BESS system connected to a balanced grid, such performances will be degraded since the occurrence of a voltage fault on the grid side. The investigation of the efficiency of the proposed strategy and its improvement during unbalanced grid conditions is a subject to be treated as future studies.

CONFLICT OF INTEREST

The authors certify that they have no conflict of interest.

ACKNOWLEDGEMENTS

None.

FINANCIAL DISCLOSURE

The authors acknowledge the financial support of the University of Hail (UOH) for the support of this work through the Research Group # RG-191245.

REFERENCES

[1] Julius AM, Patrick TG. [2019] Renewable energy injustice: The socio-environmental implications of renewable energy consumption. Energy Research & Social Science, 56: 1-11.
[2] Bensalem Y, Abbassi R, Jerbi H. [2021] Fuzzy Logic Based-Active Fault Tolerant Control of Speed Sensor Failure for Five-Phase PMSM. Journal of Electrical Engineering & Technology, 16: 287–299.
[3] Qiang W, Lina Z. [2019] Assessing the sustainability of renewable energy: An empirical analysis of selected 18 European countries, Science of The Total Environment, 692: 529-545.
[4] Destek MA, Aslan A. [2017] Renewable and non-renewable energy consumption and economic growth in emerging economies: Evidence from bootstrap panel causality. Renewable Energy, 111: 757-763.
[5] Rabeh A. Chebbi S. [2012] Energy Management Strategy for a Grid–Connected Wind-Solar Hybrid System with Battery Storage: Policy for Optimizing Conventional Energy Generation. International Review of Electrical Engineering, 7: 3979-3990.
[6] Rabeh A, Salem S, Hammami M, and Chebbi S. [2015] Analysis of renewable energy power systems: Reliability and flexibility during unbalanced network fault. Handbook of research on advanced intelligent control engineering and automation. IGI Global, pages 651–686, 2015.
[7] Hamidi F, Olteanu SC, Popescu D, Jerbi H, Dincă I, Ben Aoun S, Abbassi R. [2020] Model Based Optimization Algorithm for Maximum Power Point Tracking in Photovoltaic Panels. Energies, 13: 1-14.
[8] Abdelkader A, Rabeh A, Ali H, Diego O, Huiling C, Arslan H, Mohamed J, Mingjing W. [2020] Parameters identification of photovoltaic cell models using enhanced exploratory salp chains-based approach. Energy, 198: 117333.
[9] Hassan T, Rabeh A, Jerbi H, Mehmood K, Tahir MF, Cheema K, Elavarasan RM, Ali F, Khan IA. [2020] A Novel Algorithm for MPPT of an Isolated PV System Using Push Pull Converter with Fuzzy Logic Controller. Energies, 13, (15): 1-21.
[10] Abbassi R, Marrouchi S, Saidi S, Abbassi A, Chebbi S. [2019] Optimal Energy Management Strategy and Novel Control Approach for DPGSs Under Unbalanced Grid Faults. Journal of Circuits, Systems and Computers, 28, (04): 1950-57.
[11] Abbassi R, Hammami M, Chebbi S. [2013] Improvement of the integration of a grid-connected wind-photovoltaic hybrid system. Electrical Engineering and Software Applications, International Conference: 1-5.
[12] Marios DC, Pernille KO, Nieves E, Frederik CK, Alexis L. [2019] Economic and environmental performances of organic photovoltaics with battery storage for residential self-consumption. Applied Energy, 256: 113977.
[13] Eghtedarpour N. [2019] A synergetic control architecture for the integration of photovoltaic generation and battery energy storage in DC microgrids. Sustainable Energy, Grids and Networks, 20: 100250.
[14] Sebastian H, Rob P, Abu Abdullah M. [2019] A semi-empirical financial assessment of combining residential photovoltaics, energy efficiency and battery storage systems. Renewable and Sustainable Energy Reviews, 105: 206-214.
[15] Pietari P, Antti K, Jero A. [2021] Technical feasibility evaluation of a solar PV based off-grid domestic energy system with battery and hydrogen energy storage in northern climates. Solar Energy, 213: 246-259.
[16] Balint O, Jozsef L, [2017] Comparison of different discharge strategies of grid-connected residential PV systems with energy storage in perspective of optimal battery energy storage system sizing, Renewable and Sustainable Energy Reviews, 75: 710-718.
[17] Sushil B, Manas N. [2020] Optimal scheduling of battery storage with grid tied PV systems for trade-off between consumer energy cost and storage health, Microprocessors and Microsystems, 79: 103274.
[18] Asmae C, Mohamed T, Fouad M, Hicham M, Maya J, Abbas D, Karim A. [2020] Optimal energy management for a grid connected PV-battery system, Energy Reports, 6, (3): 218-231.
[19] Latreche S, Badoud A, Khemliche M. [2018] Implementation of MPPT algorithm and supervision of shading on photovoltaic module. Engineering, Technology & Applied Science Research, 8(6): 3541-3544.
[20] Abbassi R, Boudjemline A, Abbassi A, Torchani A, Gasmi H, Guesmi T. [2018] A numerical-analytical hybrid approach for the identification of SDM solar cell unknown parameters. Engineering Technology & Applied Science Research, 8(3): 2907-2913.
[21] Rabeh A, Sahbi M, Moez B.H, Houda J, Souad C. [2012] Voltage Control Strategy of an Electrical Network by the Integration of the UPFC Compensator. International Review On Modelling and Simulation, 5(1): 380–384.
[22] Rabeh A, Abdelkader A, Ali H, Seyedali M. [2019] An Efficient Salp Swarm-inspired Algorithm for Parameters Identification of Photovoltaic Cell Models. Energy Conversion and Management, 179: 362-372.
[23] Hao Y, Wang X, Blaabjerg F, Zhuo F. [2014] Impedance Analysis of SOGI-FLL-Based Grid Synchronization. IEEE Trans. Power Electron, 32:7409–7413.
[24] Saïdi S, Abbassi R, Chebbi S. [2014] Virtual Flux Based Direct Power Control of Shunt Active Filter. Scientica Iranica, Transaction D: Computer Science & Engineering and Electrical Engineering, 21(6): 2165-2176.

ARTICLE

MULTI-OBJECTIVE ARTIFICIAL BUTTERFLY OPTIMIZATION WITH LEVY DISTRIBUTION ALGORITHM BASED FEATURE SELECTION AND CLASSIFICATION MODEL FOR THYROID DISEASE DIAGNOSIS

Rajaram Pavithra[1*], Latha Parthiban[2]

[1]*Department of Computer Science, Bharathiyar University, TN, INDIA*
[2]*Department of Computer Science, Pondicherry University, Community College, Pondicherry, INDIA*

ISSN 0976-3104

ABSTRACT

Thyroid diseases are a commonly occurring endocrine illness over the globe, which affect the functions of thyroid gland resulting into abundant secretion of thyroid hormones. this paper presents a new feature selection (FS) based classification model for thyroid disease diagnosis using Multi-Objective Artificial Butterfly Optimization with Levy Distribution (MOABO-L) and deep neural network (DNN). The MOABOL-DNN algorithm is applied for both feature selection and tuning the training scheme of deep neural network (DNN). In order to improve the convergence rate of MOABO algorithm, Levy distribution concept is incorporated to it. The utilization of FS process helps to remove the unwanted features and increases the overall classification accuracy. For classification process, DNN with MOABO based fine-tuned training strategy is employed. To ensure the effectiveness of the MOABOL-DNN algorithm, a series of simulations takes place on two benchmark thyroid dataset. The obtained outcome indicated the goodness of the presented MOABOL-DNN technique with the maximum accuracy of 99.68% and 98.14% on the applied dataset 1 and dataset 2 respectively.

KEY WORDS
Feature selection, classification, thyroid disease, ABO algorithm, Levy flight

INTRODUCTION

The abnormal development in thyroid gland results in Congenital Hypothyroidism (CH) [1]. Globally, numerous people are infected by CH and especially in Europe and North America. Countries like Iran uses neonatal thyroid screening models for diagnosing the CH at earlier phase and treat accordingly. It is a cost-effective mechanism and Thyroid-Stimulating Hormone (TSH1) is verified within limited span; however distinct influential factors lead to cause CH even for small kids, adults, pregnant women, and genetic history of thyroid infection are also determined.

Authors [2] examined the efficiency of CH investigation and earlier remedy by correlating the Intelligence Quotient (IQ) value while examining the TSH level. Also, a statistical test with t-test and examination of covariance tests has implied the significance of earlier and massive doses of treatment in accomplishing a typical deployment in kids for CH diagnosis. Recently, Artificial Intelligence (AI) as well as Machine Learning (ML) methods was applied for achieving better interpretation of thyroid information, and medical investigation.

Diverse studies were carried out to examine the efficiency of the above mentioned models. For instance, [3] utilized the different classification models for thyroid nodule ultrasound photographs. [4] employed the two ML models for computing the structural classification of thyroid infection. Additionally, massive studies using different learning models to signify vital insights regarding thyroid disease. Under the application of ML as well as Computer Aided Diagnosis (CAD) methodologies, developers mitigate the feasible errors in diagnosing the biomedical data in both time as well as cost-efficient way. Traditionally, no classifications are deployed for CH analysis. Based on the survey, the newly developed models are highly efficient in diagnosing the thyroid disease with considerable performance.

In [5], Random Forests (RF) as well as SVM methods are trained on the ultrasound images of thyroid lumps for cancer diagnosis as benign or malignant, and maximum accuracy is attained. In [6] used Radial Basis Function (RBF), Learning Vector Quantization (LVQ), MLP, Back Propagation Algorithm (BPA), AIRS, and Perceptron frameworks for UCI dataset. In this approach, MLP and BPA have attained supreme and inferior accuracy. In [7] related the function of decision tree (DT) models in thyroid disease prediction. Moreover, NBTree is a unification of NB and DT methods which has gained better accuracy, recall and precision.

A study performed in [8] showcases that ML approaches with fundamental infrastructure for thyroid diagnosis. From the above mentioned approaches, artificial neural network (ANN) has implied optimal outcome. One of the major disadvantages of this model is that, Genetic Algorithm (GA) technique is not applicable and provides insignificant result. [9] deployed a scheme termed as Data Mining (DM) with the help of NN that is applied in early thyroid disease prediction. The system is trained under the application of BP and gradient method at the same time. However, the differences in layers of different network attributes are not applied in the training phase. [10] operated on the trial of 21 variables for training a method with the help of classification algorithm. It is trained by applying k-nearest neighbor (KNN),

Received: 22 Dec 2020
Accepted: 26 Feb 2021
Published: 9 Mar 2021

***Corresponding Author**
Email:
pave0581@gmail.com

IIOAB JOURNAL
ISSN: 0976-3104

artificial neural network (ANN) and fuzzy ANN models and compares the accuracy. It is clear that Fuzzy ANN outperforms than alternate classifiers.

This paper introduces a new feature selection based classification model for thyroid disease diagnosis using Multi-Objective Artificial Butterfly Optimization with Levy Distribution (MOABO-L) and deep neural network (DNN). The MOABOL-DNN algorithm is applied for both feature selection and tuning the training scheme of DNN. To increase the capability of the MOABO algorithm, Levy distribution concept is incorporated to it. The application of FS process helps to eliminate the unwanted features and raises the overall classification accuracy. To perform classification process, DNN with MOABO based training strategy is employed. For validating the performance of the MOABOL-DNN algorithm, a set of simulations takes place on two benchmark thyroid dataset.

METHODS

The proposed MOABOL-DNN algorithm for FS with classification processes for thyroid disease diagnosis involves three main processes namely preprocessing, feature selection, and classification. Here, MOABOL-DNN algorithm is employed for both FS and classification process. The entire workflow of the proposed MOABOL-DNN algorithm is illustrated in [Fig. 1].

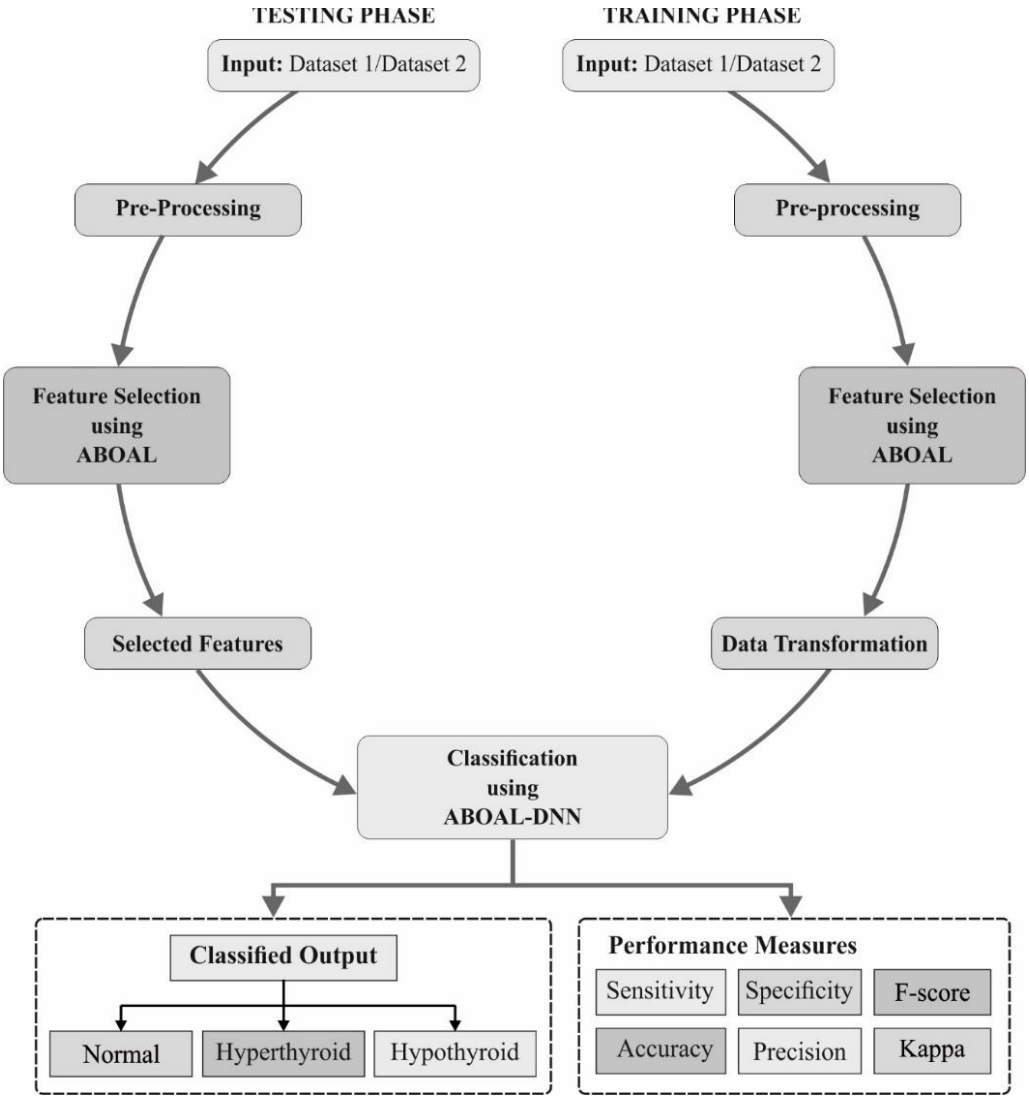

Fig. 1: Workflow of MOABOL-DNN model.

Preprocessing

In the beginning, the actual medical data is completely preprocessed to remove the unwanted noise and missing value replacement takes place via mean method. In addition, minimum-maximum (min-max) data normalization method is used to normalize the data values in the range of 0 to 1.

IIOAB JOURNAL
ISSN: 0976-3104

ABOA with Levy Flight

Based on the mate-finding principle of speckled woods, Qi et al. [11] projected a novel meta-heuristic approach named ABO. In general, the butterfly population is classified as 2 groups named sunspot and canopy. A butterfly with optimal fitness makes sunspot butterflies and remaining is referred as canopy butterflies, and various flight principles have been employed for all applications. In this framework, three flight modes are composed of ABO such as sunspot, canopy, and free flight modes.
Only few rules are developed for normalizing the mate-finding principle of butterflies in ABO approach:

- The possibility of identifying female butterflies can be increased by male butterflies where it attempts to find an optimal location called as sunspot;
- A remarkable sunspot can be accomplished when a sunspot butterfly flies towards closer sunspot;
- The canopy butterfly moves to a sunspot butterfly.

Assume that $S = \{x_1, x_2, \dots, x_N\}$ is a search space where $x_i \in \Re^n$. A multi-objective optimization issues desires to identify the global minimum $x^* \in \mathcal{S}$ which reduces a function set implied by f, i.e.:

$$x^* = \arg \min_{\forall x \in \mathcal{S}}(f(x)) = \arg \min_{\forall x \in \mathcal{S}}(f_1(x), f_2(x), \dots, f_M(x)), \quad (1)$$

subject to:

$$g_i(x) = 0 \quad \forall i = 1,2, \dots, p, \quad (2)$$

$$h_i(x) \geq 0 \quad \forall i = 1,2, \dots, q. \quad (3)$$

Collection of values satisfies the given constraints that describe the possible region and a point in this region is assumed as possible solution. In multi-objective issues, no single solution is effective interms of objectives while assuming the conflicting objects. Hence, solution for multi-objective optimization issues are not considered as a scalar value, however a collection of solutions is named as Pareto-optimal set.

Initially, the Pareto Dominance is defined as a solution vector x^a is referred as a dominative solution vector x^b $(x^a \prec x^b)$ when $(x_i^a) \leq f(x_i^b), \forall i = \{1,2, \dots, N\}$, as well as $\exists i \in \{1,2, \dots, N\}$ where $f(x_i^a) < f(x_i^b)$. Regarding the Pareto Dominance, a solution vector x^a is assumed to be a Pareto-optimal when $x^b, f_j(x^a) \leq f_j(X^b), j = 1,2, \dots, M$, and $j \in \{1,2, \dots, M\}$ in which $f_j(x^a) < f_j(x^b)$. Hence, Pareto-optimal set P^* defines the multi-objective optimization issues $f(x)$ by means of Pareto-optimal solutions are depicted as:

$$P^* = \{x \in \mathcal{S} | f(x) \prec f(x'), \forall x' \in \mathcal{S}\}. \quad (4)$$

The Pareto-optimal front PF^* by means of multi-objective optimization issues $f(x)$ and Pareto-optimal set P^* is depicted as given in the following:

$$PF^* = \{f(x) | x \in P^*\}. \quad (5)$$

Moreover, Pareto-dominance models are classified as 2 familiar classes namely, (i) indicator-related model as well as (ii) decomposition-related model.

In order to reduce the search space and avoid stagnation, levy flight concept is incorporated into the ABO algorithm. In this work, a Lévy flight plays an important role in accomplishing better results [12]. Subsequent to the massive rounds, the distance from actual walks to random walk intends to make stable distribution. Lévy flights are characterized using inverse square distribution of a step length that optimizes the random searching process if the targets become scarce in resources. Unlike, Brownian motion is more applicable when there is a requirement for placing numerous preys. The traits of 2 random walks resulted in enhancing the Swarm Intelligence (SI) optimization in which Lévy flights maximizes the eligibility of "exploration" whereas Brownian motion supports the "exploitation". Numerically, Lévy flights are considered as type of random walk with step lengths of heavy-tailed Lévy alpha-stable distribution with respect to power-law notion, $L(s) \sim |s|^{-1-\beta}$, where $0 < \beta \leq 2$ is referred as index. A common function of Lévy distribution is illustrated as

$$L(s, \gamma, \mu) = \begin{cases} \sqrt{\frac{\gamma}{2\pi}} exp\left[-\frac{\gamma}{2(s-\mu)}\right] \frac{1}{(s-\mu)^{3/2}}, & 0 < \mu < s < \infty; \\ 0, & s \leq 0. \end{cases} \quad (6)$$

Considering the $2D$-Lévy flights for sample applies a Lévy distribution whereas the directions satisfy a uniform distribution. It is pointed that, Lévy flights are highly significant in identifying unwanted and large-scale search space when compared with Brownian walk. The major cause for this discussion is that

IIOAB JOURNAL
ISSN: 0976-3104

variance of Lévy flight $\delta^2(t) \sim t^{3-\beta}, 1 \leq \beta \leq 2$ enhances robustly than Brownian random walks which is referred as, $\delta^2(t) \sim t$.

ABOA with Levy Flight based FS

In this section, the ABO-L algorithm is applied for the FS process to choose an optimal set of features. The FS problem can be considered as an optimization problem, and ABO-L algorithm can be used to resolve it. This work has presented a multi-objective FS mechanism under the application of weighted-sum technique with an aim of reducing the classification error. In mathematical format, fitness function helps the agent to accomplish optimal solution is equated as given below:

$$f = \arg \min_{\forall x \in \delta} \left(\sum_{i=1}^{M} w_i f_i(x) \right), \tag{7}$$

where $\sum_{i=1}^{k} w_i = 1$ with $w \geq 0, f_i(x)$ denotes classification error of class i, and M implies the overall class values. In addition, the extension of next technique fits the first one with tiny difference where the feature set size and classification error has to be reduced. Therefore, fitness function is projected in the following:

$$f = \arg \min_{\forall x \in \delta} \left(\sum_{i=1}^{M} w_i f_i(x) + w_{M+1} f_{M+1}(x) \right), \tag{8}$$

where $f_{M+1}(x)$ represents the count of features.

DNN based Classification

In general, DL approach is applicable for accomplishing higher level dimension features from input dataset. Next, the features are gathered from Deep Neural Network (DNN) and employed for improvising the performance efficiency [13]. Moreover, typically used DL approach is a DNN classification approach developed by the integration of stack of autoencoder (AE) with the help of SM classification technology.

In general, AE contains input, hidden and output layers. Hence, the resultant level is similar to the level of input. Furthermore, the AE is trained for embedding the input with feature spaces, where dimension is low than input space. Next, a dimension of a code space is decided as higher than input space to maximize the efficiency of classification to a greater extent. Hence, AE manages to provide best implication of input vector through the replacement of the proper code.

Hybridization of ABO-L with L-BFGS Model: Limited memory Broyden–Fletcher-Goldfarb-Shannon (L-BFGS) is referred as productive optimization method on the basis of BFGS obtained from Quasi-Newton family for high level optimizing problems. Quasi-Newton model has been developed extensively for identifying the desired models for making hessian or inverse hessian of function (f) to be limited.

The L-BFGS and BFGS use the identical approaches for generalizing a function of hessian matrix. At the initial stage, a positive definite as well as sparse symmetric matrix H_0 is obtained from f function, which is normalized. Next, H_k can be accomplished using m BFGS update to H_0 by utilizing data collected from m prior iterations when k is supreme than m. Therefore, process in L-BFGS is depicted as u_k and GD of a function is referred as gk.

$$H_{k+1} = V_k^Z H_k V_k + \rho_k s_k s_k^Z \tag{9}$$

where $\rho_k = 1/v_k^{\tau_{s_k}}, Y_k = I - \rho_{k s_k s_k^z}, s_k = u_{k+1} - u_k$ and $y_k = g_{k+1} - g_k$. The L-BFGS is suitable in resolving the computational demands because of numerous scale issues like DNN training. Additionally, L-BFGS is robust and needs lower storage for large-scale problems. To improve the exploration process of the L-BFGS, ABO-L algorithm is employed. Once the exploration is completed, L-BFGS generates better solutions and vector with iterative development where it is applied for computing general verification of proposed framework. Therefore, the inner variables of DNN architecture has been optimized using presented scheme to eliminate the local optimal issues in AEs and SM to obtain closer-optimal DNN and L-BFGS is used for local searching parameter vectors.

SM Classifier: It is a classification approach employed for multi-label classification problems. Here, the mapping is performed among input vector c with K class labels, as depicted below:

$$v_q = \frac{\exp(\theta_q^Z c)}{\sum_{k=1}^{K} \exp(\theta_k^Z c)} (q = 1, 2, \ldots K) \tag{10}$$

where $\theta_k = [\theta_{k1} \theta_{k2} \ldots \theta_{kN}]^Z$ refers the weights to be tuned using effective optimization approach.

IIOAB JOURNAL
ISSN: 0976-3104

RESULTS

For validating the performance of the MOABO-DNN model, a detailed experimentation was carried out on two benchmark two thyroid dataset [14]. A set of measures used to investigate the classification performance interms of sensitivity, specificity, precision, accuracy, F-score, and Kappa. A brief discussion of the dataset is provided in the subsequent section.

Dataset Description

The Thyroid dataset 1 includes a 3772 training and 3428 testing samples. A set of 6667 samples comes under Normal (class 3), 166 samples under hypothyroidism (Class 2), and 367 samples under hyperthyroidism (Class 1). This dataset includes a total of 21 features. Similarly, the thyroid Dataset-2 has a total of 215 Samples with 5 features and 1 target class (1 = normal, 2 = hyperthyroid, 3 = hypothyroid).

[Table 1] provides the FS results attained by the ABOL-FS with WOA-FS and SA-FS models on the applied two datasets. From the table, it is evident that, on the applied dataset 1, the ABOL-FS model has achieved excellent results with the minimum best cost of 0.567 and 0.623 on the applied dataset 1 and 2 respectively. At the same time, the SA-FS model has led to worse performance with the maximum best cost of 0.809 and 0.958 on the applied dataset 1 and 2 respectively. Though the WOA-FS model has achieved moderate results with the best cost of 0.752 and 0.914, it fails to outperform the ABOL-FS model.

Table 1: Selected Features of Existing with Proposed ABOL-FS Algorithm on Dataset-1 and Dataset-2

Methods	Dataset	Best Cost	Selected Features
ABOL-FS	Dataset-1	0.567	1,3,4,6,7,8,9,12,15,18,20
	Dataset-2	0.623	2,3,5
WOA-FS	Dataset-1	0.752	1,2,3,4,6,7,8,10,11,12,14,15,16
	Dataset-2	0.914	1,3,4
SA-FS	Dataset-1	0.809	3,5,6,7,9,10,12,13,14,15,16,18,19,20
	Dataset-2	0.958	1,2,3,5

An extensive comparative results analysis of the MABOL-DNN model with previous models is carried out with respect to distinct measures, as depicted in [Table 2] and [Figs. 2-3] [15, 16]. The resultant values verified that the MABOL-DNN model has achieved effective classifier results on the applied dataset. On comparing with existing models, the CART method has accomplished least outcome with the sensitivity of 58.8%, specificity of 59.88%, precision of 57.7%, accuracy of 58.75%, F-score of 58.32%, and kappa value of 47%. It is observed that the RT model has portrayed somewhat higher results over CART with the sensitivity of 62.5%, specificity of 65.31%, precision of 62.7%, accuracy of 62.5%, F-score of 63.01%, and kappa value of 52.3%. It is noticeable that the J48 model has realized somewhat practicable outcome with the sensitivity of 63.8%, specificity of 68.51%, precision of 58.1%, accuracy of 66.25%, F-score of 69.02%, and kappa value of 56.8%. In line with, the NBTree model has reached to reasonable outcome with the sensitivity of 75%, specificity of 76.43%, precision of 77%, accuracy of 75%, F-score of 70.12%, and kappa value of 68%. At the same time, the IGWO-RBF-SVM model has led to moderate results with the sensitivity of 78.90%, specificity of 81.17%, precision of 68.79%, accuracy of 78.49%, F-score of 65.90%, and kappa value of 61.98%. On continuing with, even better performance with the sensitivity of 81.17%, specificity of 75.18%, precision of 72.71%, accuracy of 79.11%, F-score of 67.23%, and kappa value of 62.65% has been attained by the IGWO-ANN model. Moreover, the IGWO-Linear-SVM model has obtained a sensitivity of 82.58%, specificity of 90.46%, precision of 70.69%, accuracy of 93.96%, F-score of 71.83%, and kappa value of 64.32%. Besides, somewhat acceptable outcome is provided by the IGWO-MSVM model with the sensitivity of 94.65%, specificity of 94.5%, precision of 91.83%, accuracy of 97.49%, F-score of 91.76%, and kappa value of 90.65%.

Table 2: Result analysis of existing with proposed MOABOL-DNN method on thyroid dataset

Methods	Sensitivity	Specificity	Precision	Accuracy	F-score	Kappa
MOABOL-DNN (Dataset-1)	**97.75**	**99.54**	**95.39**	**99.68**	**96.50**	**95.73**
MOABOL-DNN (Dataset-2)	**96.16**	**98.90**	**94.27**	**98.14**	**95.16**	**93.58**
DNN (Dataset-1)	96.54	98.32	94.22	98.04	94.92	93.84
DNN (Dataset-2)	95.13	96.48	92.89	97.09	93.12	91.90
IGWO+MSVM	94.65	94.50	91.83	97.49	91.76	90.65
IGWO+Linear-SVM	82.58	90.46	70.69	93.96	71.83	64.32
IGWO+RBF-SVM	78.90	81.17	68.79	78.49	65.90	61.98
IGWO+ANN	81.17	75.18	72.71	79.11	67.23	62.65
NBTree	75.00	76.43	77.00	75.00	70.12	68.00
J48	63.80	68.51	58.10	66.25	69.02	56.80
Rand. Forest	65.00	69.06	66.00	65.00	66.87	55.10
Rand. Tree	62.50	65.31	62.70	62.50	63.01	52.30
CART	58.80	59.88	57.70	58.75	58.32	47.00

IIOAB JOURNAL
ISSN: 0976-3104

Similarly, the D-KELM model has obtained moderate results on the dataset 2 with the sensitivity of 84.21%, specificity of 94.9%, precision of 78.31%, accuracy of 94.04%, F-score of 75.17%, and kappa value of 70.68%. Eventually, the D-KELM model on the dataset 1 has resulted to a somewhat sensible outcome with the sensitivity of 87.53%, specificity of 95.56%, precision of 79.08%, accuracy of 94.06%, F-score of 76.5%, and kappa value of 72.89%. Instantaneously, the OD-KELM model has showcased somewhat better results on the dataset 2 over all the other methods by realizing sensitivity of 86.79%, specificity of 96.19%, precision of 83.1%, accuracy of 94.11%, F-score of 84.78%, and kappa value of 79.93%. Next to that, the OD-KELM model has established reasonable results on the dataset 1 with the sensitivity of 92.67%, specificity of 97.88%, precision of 79.37%, accuracy of 98.01%, F-score of 83.98%, and kappa value of 78.29%.

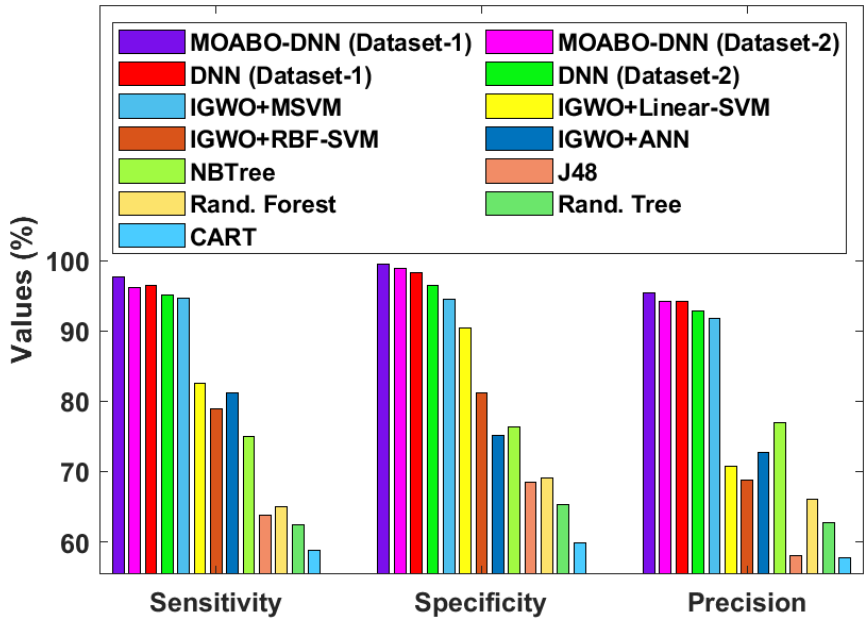

Fig. 2: Comparative result analysis of MOABO-DNN with other Models-I.

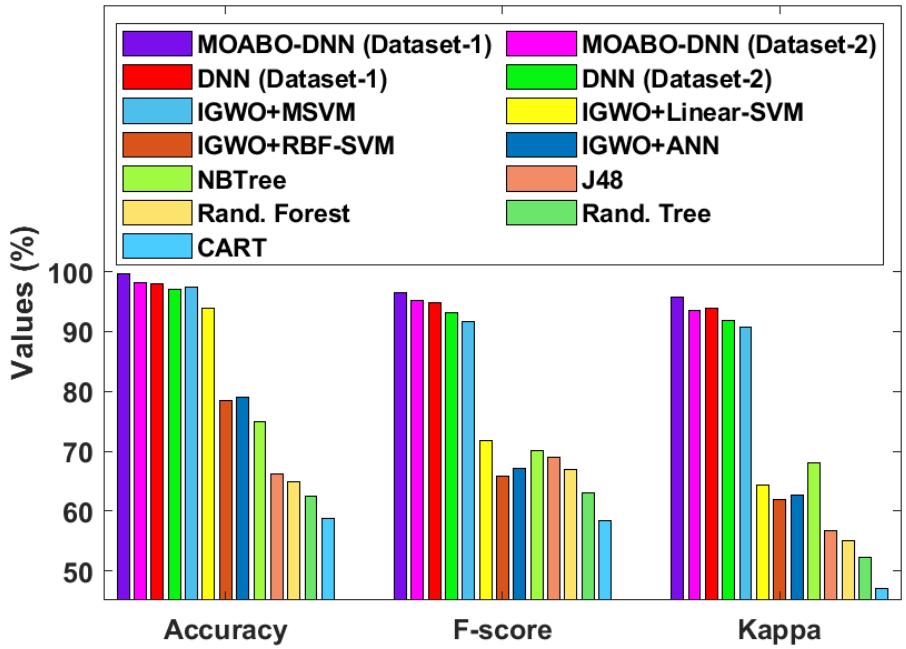

Fig. 3: Comparative result analysis of MOABO-DNN with other models-II.

However, the MOABOL-DNN model has accomplished superior results over the compared methods with the maximum sensitivity of 96.16%, specificity of 98.90%, precision of 94.27%, accuracy of 98.14%, F-score of 95.16%, and kappa value of 93.58%. On continuing with, the MOABOL-DNN model has resulted to

IIOAB JOURNAL
ISSN: 0976-3104

effective classification on dataset 2 with the highest sensitivity of 96.16%, specificity of 98.90%, precision of 94.27%, accuracy of 98.14%, F-score of 95.16%, and kappa value of 93.58%. After observing the tables and resultant figures, it is apparent that the MOABOL-DNN model has achieved better results on the diagnosis of thyroid with the maximum accuracy of 99.68% and 98.14% on the applied dataset 1 and dataset 2 respectively. Therefore, it can be applied as a novel diagnostic tool for thyroid diseases.

CONCLUSION

This paper has developed a FS based classification model using MOABOL-DNN and DNN for thyroid disease diagnosis. The proposed MOABOL-DNN algorithm for FS with classification processes for thyroid disease diagnosis involves three main processes namely preprocessing, feature selection, and classification. Here, MOABOL-DNN algorithm is employed for both FS and training scheme tuning of DNN. Initially, data preprocessing takes place to transform the raw data into a useful format. Then, MOABOL based FS process is executed to select an optimal number of features. Finally, DNN model is employed for classification and MOABOL-DNN algorithm is applied to fine tune the training process. For assuring the superior performance of the MOABOL-DNN algorithm, a set of simulations takes place on two benchmark thyroid dataset. The simulation outcomes ensured the effective diagnosis results with the maximum accuracy of 99.68% and 98.14% on the applied dataset 1 and dataset 2 respectively. In future, the performance of the MOABOL-DNN algorithm can be improved by clustering techniques.

REFERENCES

[1] Hashemipour M, Soheilipour F, Karimizare S, Khanahmad H, Karimipour M, Aminzadeh S, Kokabee L, Amini M, Hovsepian S, Hadian R. [2012] Thyroid peroxidase gene mutation in patients with congenital hypothyroidism in Isfahan, Iran. International journal of endocrinology.

[2] Najmi SB, Hashemipour M, Maracy MR, Hovsepian S, Ghasemi M. [2013] Intelligence quotient in children with congenital hypothyroidism: The effect of diagnostic and treatment variables. Journal of research in medical sciences: the official journal of Isfahan University of Medical Sciences. 18(5):395.

[3] Singh N, Jindal A. [2012] A segmentation method and comparison of classification methods for thyroid ultrasound images. International Journal of Computer Applications. (11):43-9.

[4] Erol R, Oğulata SN, Şahin C, Alparslan ZN. [2008] A radial basis function neural network (RBFNN) approach for structural classification of thyroid diseases. Journal of medical systems. 32(3):215-20.

[5] Prochazka A, Gulati S, Holinka S, Smutek D. [2019] Classification of thyroid nodules in ultrasound images using direction-independent features extracted by two-threshold binary decomposition. Technology in cancer research & treatment. 18:1533033819830748.

[6] Maysanjaya IM, Nugroho HA, Setiawan NA. [2015] A comparison of classification methods on diagnosis of thyroid diseases. In2015 International seminar on intelligent technology and its applications (ISITIA). 89-92.

[7] Turanoglu-Bekar E, Ulutagay G, Kantarcı-Savas S. [2016] Classification of thyroid disease by using data mining models: a comparison of decision tree algorithms. Oxford Journal of Intelligent Decision and Data Sciences. 2:13-28.

[8] Razia S, Rao MN. [2016] Machine learning techniques for thyroid disease diagnosis-a review. Indian J Sci Technol. 9(28):10-7485.

[9] Prerana PS, Taneja K. [2015] Predictive data mining for diagnosis of thyroid disease using neural network. International Journal of Research in Management, Science & Technology. 3(2):75-80.

[10] Umadevi S, JeenMarseline KS. [2017] Applying classification algorithms to predict thyroid disease. Int J Eng Sci Comput. 7(10):15118-20.

[11] Qi X, Zhu Y, Zhang H. [2017] A new meta-heuristic butterfly-inspired algorithm. Journal of computational science. 23:226-39.

[12] Li D. [2014] Cooperative quantum-behaved particle swarm optimization with dynamic varying search areas and Lévy flight disturbance. The scientific world journal.

[13] Pustokhina IV, Pustokhin DA, Gupta D, Khanna A, Shankar K, Nguyen GN. [2020] An effective training scheme for deep neural network in edge computing enabled Internet of medical things (IoMT) systems. IEEE Access. 8:107112-23.

[14] Dataset Source: https://archive.ics.uci.edu/ml/datasets/Thyroid+Disease

[15] Shankar K, Lakshmanaprabu SK, Gupta D, Maseleno A, De Albuquerque VH. [2020] Optimal feature-based multi-kernel SVM approach for thyroid disease classification. The journal of supercomputing. 76(2):1128-43.

[16] Turanoglu-Bekar E, Ulutagay G, Kantarcı-Savas S. [2016] Classification of thyroid disease by using data mining models: a comparison of decision tree algorithms. Oxford Journal of Intelligent Decision and Data Sciences. 2:13-28.

ARTICLE

MEDICAL AND BIOLOGICAL FEATURES OF RAW MATERIAL RESOURCES OF THE YAKUTIAN HORSE

Maria Nikolaevna Pak*, Valentina Tikhonovna Vasilyeva, Revoriy Vasilievich Ivanov, Leonid Nikolaevich Vladimirov, Nikolay Vasilievich Vinokurov

Yakutsk Scientific Research Institute of Agriculture named after M.G. Safronov, Bestuzhev-Marlinsky Street, 23, bld. 1, Yakutsk, RUSSIA

ISSN 0976-3104

ABSTRACT

Since ancient times, the inhabitants of the Far North have developed a "northern" type of metabolism, where the predominance of protein/fat components in food is necessary, rather than carbohydrates. The Republic of Sakha (Yakutia) has significant potential for rationalizing nutrition, taking into account protein/lipid metabolism and the physiological needs of a person living in extreme conditions of the North, through the production of meat products from local raw materials. Isolation of lipids from fat samples was carried out according to Folch's method. Determination of the composition of fatty acids was carried out using gas-liquid chromatography. Determination of the biochemical composition of blood was carried out using infrared spectroscopy and infrared drying. The Yakutian horse meat is unique due to its high energy content, the balanced amino acid composition of proteins, the content of vitamins, and the presence of bioactive substances, including polyunsaturated fatty acids. The highest percentage of polyunsaturated fatty acids is found in the internal fat and equals 27.3%, the optimal composition of polyunsaturated fatty acids is found in the kidney suet equaling 24.95%, and abdominal fat has a low content of polyunsaturated fatty acids (21.03%). It is worth noting that of all the studied samples of fat from different parts of the carcass, only the inner fat showed the highest content of γ- and α-linolenic fatty acids. The authors carried out work to obtain a concentrate from the fat of a Yakutian horse as a raw material for a food additive. The dry blood of Yakutian horses contains a whole range of biologically active substances. The research results indicate that the raw materials of the Yakutian horse have a high biological value and can be used to obtain specialized food products. The results obtained allow the authors to conclude that the products of the Yakutian horse breeding fully meet the nutritional requirements and, with proper planning, can provide the population with protein/fat food. The meat, internal fat, and blood of the Yakutian horse can be used as a preventive product to compensate for the deficiency of animal protein, polyunsaturated fatty acids, and iron and as a raw material for obtaining specialized food products.

KEY WORDS
Yakutian horse, horse meat, foal meat, subcutaneous fat, internal fat, polyunsaturated fatty acids, dry blood, proteins, organic iron.

INTRODUCTION

One of the fundamental bases for the formation of human health is the nutritional factor. It has been established that the "northern" type of metabolism requires the predominance of protein/fat components in food [1-3]. In the North, in humans, the energy role of carbohydrates decreases, and the role of fats and, to a lesser extent, proteins increases; the so-called polar metabolic type is formed [1]. According to Steegmann [2], in aboriginal people living in cold climates, the increased basal metabolic rates appear to be genetically induced. During exposure to cold, the body controls heat storage through well-known channels but also specialized thermogenic functions, such as metabolism in brown adipose tissue [3]. Snodgrass et. al. [3] studied the basal metabolic rates (BMR) in the Yakuts, an indigenous high-latitude population from the Sakha Republic of Russia. It was found that the Yakuts had an increased BMR. The results obtained suggest the possibility of a genetic or evolutionary mechanism [3]. The inhabitants of the Far North need an increased amount of fat — up to 140 g per day (36% of the calorie content of 3,500 kcal), and 60-90% of them should be represented by animal fats, given the specificity of northern sources of animal proteins and fats [4, 5]. It has now been established that in the diet of northerners, there are some violations in the principles of rational nutrition: in energy balance and balance in basic nutrients, proteins, fats, carbohydrates, vitamins, and minerals [1]. Katyukhin et al. (2004) have shown that in the Russian Arctic, cerebrovascular accidents are the most common diseases of the cardiovascular system [6]. According to the "Strategy of socio-economic development of the North-West Federal District for the period up to 2020", the development of the agro-industrial complex should be aimed at the formation of food resources, meeting the needs of the population of the district in affordable and high-quality Russian-produced food products following the recommended rational norms of food consumption. Under this strategic direction in the development of the agro-industrial complex of the regions of the Far North, the main goal should be an increase in production volumes to ensure regional food security, and the development of production of local products. Dairy and beef cattle breeding, pig breeding, poultry farming, etc. will be of the biggest importance in the development of the agro-industrial complex [7].

The Republic of Sakha (Yakutia) has significant potential for rationalizing nutrition, taking into account protein/lipid metabolism and the physiological needs of a person living in extreme conditions of the North, through the production of meat products from local raw materials. In the traditional Yakut cuisine, horse meat, beef, venison, game birds, as well as offal and blood, are traditionally used for food. A distinctive feature of Yakut cuisine is the fullest possible use of all components of the original product. Almost all by-products are actively used. In particular, offal soups, blood delicacies, etc. are very popular. Frozen meat and fish are used to make stroganina (frozen meat or fish cut into thin slices); beef or horse blood is used to make khaan (Yakut blood sausage) [8].

Received: 12 Nov 2020
Accepted: 28 Dec 2020
Published: 24 Mar 2021

***Corresponding Author**
Email:
pak-maria@list.ru

IIOAB JOURNAL
ISSN: 0976-3104

The Yakutian horse meat is unique due to its high energy content, the balance of the amino acid composition of proteins, the content of vitamins, the presence of bioactive substances, and high digestibility. In addition to meat carcasses, several other slaughter products are obtained during the primary processing of horses, such as by-products (internal fat, blood, intestinal raw materials, etc). Many of them are not fully utilized, although they could represent a valuable raw material for the food and processing industry. The products of northern animals, including meat of horse breeds bred in Yakutia, have a high nutritional value and contain more proteins, fats, minerals, vitamins, and biologically active substances than meat from animals bred in southern latitudes [9]. The high quality of the meat of Yakutian horses is conditioned by the peculiarity of the accumulation of nutrients in the fodder plants of the North. For the Yakuts, the meat of the Yakutian horse has long been a favorite food, from which more than 80 different meat dishes with high nutritional value are prepared. In Yakut traditional cuisine, horse meat is often eaten as stroganina (frozen and cut into slices), or boiled and fried [8].

In this article we analyzed the medical and biological aspects of food products made from various raw materials of the Yakutian horse.

MATERIALS AND METHODS

When conducting the research, ethical standards in relation to animals were observed and approved by the commission of the Yakutsk Scientific Research Institute of Agriculture named after M.G. Safronov. The work was carried out in the laboratory of selection and breeding of horses of the Yakutsk Scientific Research Institute of Agriculture named after M.G. Safronov. The studies were carried out on the slaughter products of the Yakutian breed of horses. The most important points were the calorie content of meat and the biochemical composition of by-products (subcutaneous and internal fat) and slaughter blood (mass fraction of proteins and minerals). The collection of raw materials was carried out directly during slaughter. Raw materials were subjected to immediate freezing by natural cold and freshly delivered to the place of processing within 24 hours in dark packaging.

For the study, we took fat samples of the Yansky and indigenous types of the Yakut breed from the following parts of the carcass: subcutaneous, internal, cervical, and abdominal. Fat samples were taken during the mass slaughter of horses when a stable low temperature of -20 to -30ºC was reached at the end of October – the beginning of November. Immediately after slaughter, fatty raw materials were cleaned of contaminants, blood clots, and muscle tissue and frozen at a temperature of -25 to -30°C. To isolate fat from raw fat, we chose the low-temperature method. The low-temperature method of obtaining fat has the following technological parameters: grinding fat at a temperature of -10 to -5 °C to particles with a size of 3-4 mm, centrifugation at 3,000 rpm for 45 minutes, followed by separation [7]. The determination of the composition of fatty acids was carried out in the laboratory of the All-Union Scientific Research Institute of the Meat Industry named after V.M. Gorbatov. Isolation of lipids from the samples was carried out using extraction with chloroform/methanol according to Folch's method. The purity of the isolated lipids was checked using thin-layer chromatography. The determination of the composition of fatty acids was carried out using an HP 6890 gas chromatograph (Hewlett Packard) [11, 14]. Blood samples for food purposes were taken only from healthy animals. Slaughter blood was prepared in stationary conditions at blood collection points in special standard polymer containers with a volume of 250 and 500 ml. Each blood batch was defibrinated before analysis.

Studies of the biochemical composition of blood were carried out at the accredited testing center of the All-Union Scientific Research Institute of the Meat Industry named after V.M. Gorbatov in accordance with GOST 30178-96 [11]. Drying was carried out using infrared drying to ensure maximum preservation of the properties and biological value of blood proteins. Complete drying of blood using infrared radiation was achieved after 2 hours and 20 minutes. To determine macro and microelements, whole blood was dried at a temperature of 70 to 80˚C and the dried blood was ground in a mill.

Statistical data processing was carried out using the Excel for Windows XP 2002 software package and was expressed as M±m. The degree of reliability of the revealed differences was determined using Student's t-test.

RESULTS AND DISCUSSION

The Yakutian horse is distinguished by a high slaughter yield and meat yield from the carcass. Yakutian horses, depending on age, after autumn grazing and fattening, have the following average carcass weight: 102.3 kg at 6 months of age, 165 kg at 2.5 years, and 228 kg when they are fully grown. Their slaughter yield equals 55.8, 49.1, and 55.5% respectively [9]. The live weight of 6-month-old foals varies considerably depending on the type and breed. If the Yansky type of the Yakutian breed weighs on average 170.23 kg, then the foals of the Prilensky breed weigh 215.6 kg. Foals of the Kolyma type of the Yakutian breed are distinguished by a high content of internal fat (11.3 kg), while in foals of other types and breeds it ranges from 4.7 to 6.0 kg.

The minimum slaughter yield is observed in young animals of 2.5 years, especially in the indigenous (46.3%) and Yansky (46.48%) types of the Yakutian breed.

IIOAB JOURNAL
ISSN: 0976-3104

Depending on the fatness category, the calorie content of 1 kg of meat from Yakutian horses ranges from 1,922 to 2,724 kcal. The chemical composition of meat and its caloric content largely depends on the category of horse nutrition rather than age and gender.

Currently, about 80% of the meat of the Yakutian horse is produced from the meat of foals at the age of six months. From the data presented in Table 1, it can be seen that the meat of foals of the Prilensk breed and the Kolyma type had the highest calorie content (2,415 and 2,536 kcal). The highest fat content is observed in the meat of the Prilensk and Kolyma type foals — 18.4 and 17.1%. The meat of foals, in addition to the Yansky type, contained almost the same amount of protein (from 17.2 to 18.6%). The meat of the Prilensk foals contained a greater amount of phosphorus.

Table 1: Chemical composition and energy value of meat of 6-month-old foals of the Yakutian horse [9]

Indicators	Prilensk breed	Megezhek breed	Yakutian breed			Average for the Yakutian horse
			Root type	Yansky type	Kolyma type	
Moisture, %	62.8	67.9	65.0	67.6	62.9	65.2
Fat, %	18.4	12.7	16.4	14.7	17.1	16.0
Protein, %	17.2	18.0	17.3	16.3	18.6	17.2
Ash, %	1.6	1.4	1.4	1.4	1.4	1.4
Calcium, %	0.13	0.09	0.11	0.10	0.13	0.11
Phosphorus, %	0.37	0.29	0.28	0.26	0.29	0.28
Caloric content of 1 kg of meat, kcal	2,415	1,922	2,235	2,027	2,536	2,197

Based on the Table 1, it can also be noted that the chemical composition and energy value of foals depend on the breed and types of horses.

Yakutian horse offal is one of the favorite delicacies of the Yakuts. Dozens of dishes are prepared from offal, including high-quality products. Subcutaneous and internal fats obtained from horse meat and foal meat of the Yakutian horse are of no small interest in terms of by-products. The fat yield, depending on the age, breeds, and types of the Yakutian horse, varies within the following range: older mares weigh up to 23.06 kg, young horses of 2.5 years weigh 6.37-9.70 kg, and 6-month-old foals weigh 4.68-5.75 kg. The fat of the Yakutian horse is represented by a unique composition. Fat has high digestibility, low melting point and surpasses other farm animals in the content of fatty acids of the omega-3 and omega-6 classes, which are essential fatty acids since they are not synthesized in the human body. Cholesterol and unsaturated fatty acid fraction are in the most beneficial balanced state.

Polyunsaturated fatty acids (PUFAs), which are of particular importance for maintaining normal human health, are of great practical interest. The high biological value of PUFAs is as follows: they are the structural components of the lipids of the body cells. The presence of PUFAs determines the biological activity of phospholipids and the properties of biological membranes. They have an anti-atherosclerotic effect: an increase in the excretion of cholesterol from the body, a decrease in the formation of low-density lipoproteins, an increase in elasticity, and a decrease in the permeability of the vascular wall. They are substrates for the synthesis of prostaglandins, thromboxanes, leukotrienes, and eicosanoids — powerful intracellular regulators of the functioning of almost all body systems: in the regulation of immune genesis and hemostasis and the development of inflammatory, allergic, and proliferative reactions [10].

As a result of our studies of the fat of the Yakutian horse, we found that fats from different parts of the carcass differ in the composition of fatty acids. The highest percentage of PUFAs is found in the internal fat and equals 27.3%, the optimal composition of PUFAs is found in the kidney suet equaling 24.95%, and abdominal fat has a low content of PUFAs (21.03%). It is interesting to note that of all the studied samples of fat from different parts of the carcass, only the internal fat was found to have the highest content of γ- and α-linolenic fatty acids. In our previous studies, it was noted that deer and pork fats were inferior in terms of γ- and α-linolenic fatty acids to the fat of a horse of the Yakutian breed. Besides, when comparing the fat of a Yakutian horse with deer and pork fat, it was noted that horse fats were distinguished by a relatively low content of saturated acids and a higher level of PUFAs [11].

In general, it can be noted that the fat of the Yakutian breed horse, especially the internal fat, in its fatty acid composition differs from similar fats of slaughter animals and is the closest in the presence of omega-3 fatty acids to the fats of inhabitants of cold sea waters. After studying the biochemical composition of the fat of the Yakutian horse, we carried out work on obtaining a concentrate from the fat of the Yakutian horse as a raw material for a food additive to obtain fat-containing raw materials with PUFAs.

The results of work on the extraction of concentrate from the fat of a horse of the Yakut breed are secured by the patent for invention No. 2538367 RF. We developed technical specifications (TU) and technological instructions for the document TU 9215-036-00670203-2013 "Internal fat of the Yakutian breed horse". The internal fat of a horse of the Yakut breed can serve as a valuable raw material for the production of

IIOAB JOURNAL
ISSN: 0976-3104

food products and prophylactic preparations for humans as a source of PUFAs, as well as biologically active food additives with an effective method of extracting them from raw fat.

Based on the results of the research, a technological process for obtaining new types of products from the fat of the Yakutian horse may be developed.

Slaughter blood is also a valuable raw material for obtaining specialized food products. It can serve as a source of nutrients and biologically active substances, including high-value protein and organic iron [12]. The biological value of blood is that in terms of the content of protein substances it is equal to meat, so the meat of a Yakutian horse contains 17.0-19.7% of proteins, and the level of proteins in horse blood reaches 18% [13]. The content of a complex of all substances necessary for the normal functioning of the body in the blood indicates the possibility of its use not only as food raw material but also as a valuable therapeutic agent. The composition and properties of horse blood in terms of biochemical composition, including amino acid and mineral composition, are not inferior to the blood of other slaughter animals; in some respects, they even exceed it [14].

The presence of a significant amount of iron in the horse's blood predetermines its use for the production of food products that contribute to the prevention and treatment of iron deficiency conditions, to which a significant part of the population is exposed. Therefore, as a dietary product, horse blood can be used in case of anemia, general weakness, growth retardation, and a lack of nutrition to restore protein reserves [15].

The dynamics of the protein content in the dry blood of mares depend mainly on the age and physiological state. According to Fig. 1, the largest mass fraction of protein is observed in the blood of 8-year-old mares, and the smallest mass fraction is found in the blood of mares of 12-15 years. It should be noted that there are no significant fluctuations in the mass fraction of blood protein since all studied animals of the same contingent are sexually mature mares 8-19 years old.

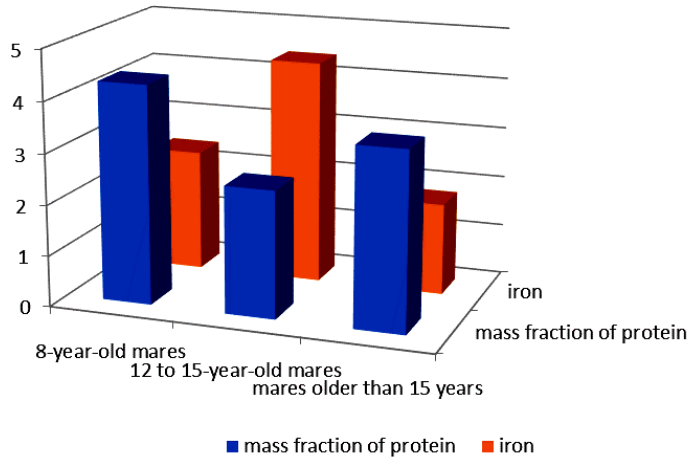

Fig. 1: Mass fraction of protein and minerals in the blood of the Yakutian horse depending on age

The iron content in the dry blood of Yakutian horses varies insignificantly from 220.95 to 234.61 mg/kg, which indicates a stable level of supply of the horses with this element. The dry blood of Yakutian horses effectively affects the human body due to a whole complex of biologically active substances. It contains peptides, amino acids, hormones, nucleotides, minerals, and vitamins. The high iron content in the blood makes it a promising raw material for the production of dietary supplements as an additional source of iron, iron-containing preparations, and specialized food products. We have developed TU 9215-038-00670203-2013 "Dry blood of Yakutian breed horses". In the laboratory center of the All-Union Scientific Research Institute of the Meat Industry named after V.M. Gorbatov, tests were carried out to verify compliance with the requirements of technical specifications for physical, chemical, microbiological, and safety indicators.

CONCLUSION

The research results indicate that the raw material resources of the Yakutian horse have a high biological value and can be used to obtain specialized food products. The results obtained allow us to conclude that the products of the Yakutian horse breeding fully meet the above requirements, and with proper planning, they can provide the population with protein and fat food. The meat, internal fat, and blood of the Yakutian horse can be used as a preventive product to compensate for the deficiency of animal protein, PUFAs, and iron and as a raw material for obtaining specialized food products.

IIOAB JOURNAL
ISSN: 0976-3104

CONFLICT OF INTEREST

There is no conflict of interest.

ACKNOWLEDGEMENTS

None.

FINANCIAL DISCLOSURE

None.

REFERENCES[#]

[1] Golubchikov SN, Khimenkov AN, Erokhin SV. [2003] Mediko-ekologicheskie problemy uluchsheniya zhiznennoi sredy severyan [Medical and ecological problems of improving the living environment of the northern population]. Energiya. 4: 54-57.

[2] Steegmann AT Jr. [2007]. Human cold adaptation: an unfinished agenda. Am J Hum Biol. 19(2): 218–227.

[3] Snodgrass JJ, Leonard WR, Tarskaia LA, Alekseev VP, Krivoshapkin VG. [2005] Basal metabolic rate in the Yakut (Sakha) of Siberia. Am J Hum Biol. 17(2): 155-172.

[4] Eganyan RA. [2013] Osobennosti pitaniya zhitelei Krainego Severa Rossii (obzor literatury) [Nutritional features of the residents of the Far North of Russia (literature review)]. Profilakticheskaya meditsina. 16(5): 41-47.

[5] Bang HO, Dyeberg J. [1980] Lipid metabolism and ischemic heart disease in Greenland Eskimos. Adv. in nutritional research. N.Y.: Plenum Press: 1-22.

[6] Katyukhin VN, Grigoruk SD, Lyuks NV, Karpin VA. [2004] Klimatoekologicheskie faktory riska ostrogo infarkta miokarda v usloviyakh Krainego Severa [Climatic and ecological risk factors for acute myocardial infarction in the Far North]. Kardiologiya. 2: 61-64.

[7] Strategiya sotsialno-ekonomicheskogo razvitiya Severo-Zapadnogo federalnogo okruga na period do 2020 goda. Utverzhdena Pravitelstvom RF No.2074-r [Strategy of socio-economic development of the North-West Federal District for the period up to 2020. Approved by the Government of the Russian Federation as document No. 2074-p]. November 18, 2011. Retrieved from: https://rg.ru/pril/62/64/23/2074_strategiia.pdf

[8] Rodionov TP. [1997] Natsionalnaya kukhnya: dorogu dobrym traditsiyam [National cuisine: the road to good traditions]. Ilin. 1: 48-49.

[9] Abramov AF, Ivanov RV, Alekseev ND. [2013] Myasnaya produktivnost i kachestvo myasa porol loshadei, razvodimykh v Yakutii [Meat productivity and meat quality of the horse breeds bred in Yakutia]. Yakutsk: Ofset.

[10] Köhler-Forsberg O, Benros ME. [2018] Efficacy of Anti-Inflammatory Treatment in Depression. Inflammation and Immunity in Depression. Basic Science and Clinical Applications. 30: 525-538.

[11] Slobodchikova MN, Vasileva VT, Ivanov RV. [2018] Novye aspekty bezotkhodnogo ispolzovaniya vtorichnogo syrya konevodstva v Yakutii [New aspects of waste-free use of secondary raw materials for horse breeding in Yakutia]. Voprosy pitaniya. 87(4): 87-92.

[12] Ofori J, Hsieh Y-H. [2014] Issues Related to the Use of Blood in Food and Animal Feed. Critical reviews in food science and nutrition. 54(5): 687-697.

[13] Caldironi HA, Ockerman, HW. [1982] Incorporation of blood proteins into sausage. J Food Sci. 47(2): 405-408.

[14] Vasileva VT, Ivanov RV, Slobodchikova MN, Vasileva RE, Stepanov KM. [2015] Issledovaniya v oblasti pererabotki vtorichnogo syrya tabunnogo myasnogo konevodstva [Studies in the field of processing of secondary raw materials of herd meat horse breeding]. Voprosy pitaniya. 84(S3): 92.

[15] Luneva RA, Loretts OG, Makoveeva AS, Tsyganova OS. [2014] Tekhnologiya pervichnoi pererabotki produktov zhivotnovodstva [Technology of primary processing of animal products]. Ekaterinburg.

[#] *English translations of the references are presented.*